Water Research 123 (2017) 153–161

Contents lists available at ScienceDirect

Water Research

journal homepage: www.elsevier.com/locate/watres

Oxidation of β-lactam antibiotics by peracetic acid: Reaction kinetics, product and pathway evaluation

Kejia Zhang [a, b], Xinyan Zhou [a], Penghui Du [b, c], Tuqiao Zhang [a], Meiquan Cai [b, d], Peizhe Sun [b, e], Ching-Hua Huang [b, *]

[a] College of Civil Engineering and Architecture, Zhejiang University, Hangzhou, 310058, People's Republic of China
[b] School of Civil and Environmental Engineering, Georgia Institute of Technology, Atlanta, GA, 30332, United States
[c] Institute of Process Engineering, Chinese Academy of Sciences, Beijing, 100190, People's Republic of China
[d] School of Environment, Tsinghua University, Beijing, 100084, People's Republic of China
[e] School of Environmental Science and Engineering, Tianjin University, Tianjin, 300072, People's Republic of China

A R T I C L E I N F O

Article history:
Received 24 April 2017
Received in revised form
15 June 2017
Accepted 21 June 2017
Available online 22 June 2017

Keywords:
Peracetic acid
Penicillins
Cephalosporins
Emerging contaminants
Wastewater treatment
Oxidation

A B S T R A C T

Peracetic acid (PAA) is a disinfection oxidant used in many industries including wastewater treatment. β-Lactams, a group of widely prescribed antibiotics, are frequently detected in wastewater effluents and surface waters. The reaction kinetics and transformation of seven β-lactams (cefalexin (CFX), cefadroxil (CFR), cefapirin (CFP), cephalothin (CFT), ampicillin (AMP), amoxicillin (AMX) and penicillin G (PG)) toward PAA were investigated to elucidate the behavior of β-lactams during PAA oxidation processes. The reaction follows second-order kinetics and is much faster at pH 5 and 7 than at pH 9 due to speciation of PAA. Reactivity to PAA follows the order of CFR ~ CFX > AMP ~ AMX > CFT ~ CFP ~ PG and is related to β-lactam's nucleophilicity. The thioether sulfur of β-lactams is attacked by PAA to generate sulfoxide products. Presence of the phenylglycinyl amino group on β-lactams can significantly influence electron distribution and the highest occupied molecular orbital (HOMO) location and energy in ways that enhance the reactivity to PAA. Reaction rate constants obtained in clean water matrix can be used to accurately model the decay of β-lactams by PAA in surface water matrix and only slightly overestimate the decay in wastewater matrix. Results of this study indicate that the oxidative transformation of β-lactams by PAA can be expected under appropriate wastewater treatment conditions.

1. Introduction

Peracetic acid (PAA), the peroxide of acetic acid, is commonly used as a disinfectant in various industries. The global usage of PAA was estimated around 170 kt in 2013 (Luukkonen and Pehkonen, 2017). PAA can be produced by the reaction of acetic acid with hydrogen peroxide (H_2O_2) in the presence of a strong acid catalyst such as sulfuric acid (Zhao et al., 2007). Commercially available PAA is sold as a quaternary equilibrium mixture containing PAA, H_2O_2, acetic acid and water, as shown in Equation (1) below:

$$CH_3C(=O)OH + H_2O_2 \leftrightarrow CH_3C(=O)OOH + H_2O \quad (1)$$

The oxidation potential of PAA was reported around 1.76 V (Awad et al., 2004), higher than aqueous chlorine (1.48 V) and chlorine dioxide (1.28 V) but lower than ozone (2.08 V) and ferrate(VI) (2.2 V) (Luukkonen and Pehkonen, 2017; Sharma et al., 2016). The undissociated acid ($CH_3C(=O)OOH$) is considered the biocidal or oxidation form of PAA. In the typical pH range of water treatment, PAA may undergo acid-base speciation with a dissociation constant (pK_a) around 8.2 (Yuan et al., 1997a), according to Equation (2):

$$CH_3C(=O)OOH + H_2O \leftrightarrow CH_3C(=O)OO^- + H_3O^+ \quad pKa = 8.2 \quad (2)$$

The conjugate acid, conjugate base, and nonspecified form of peracetic acid are denoted herein as PAAH, PAA^-, and PAA, respectively.

PAA is known for its bactericidal, virucidal, fungicidal and sporicidal effects. Its broad spectrum antimicrobial activity renders the applications of PAA in various industries including food processing, beverage, medical, pharmaceutical, pulp and paper, and

* Corresponding author.
E-mail address: ching-hua.huang@ce.gatech.edu (C.-H. Huang).

http://dx.doi.org/10.1016/j.watres.2017.06.057
0043-1354/© 2017 Published by Elsevier Ltd.

textile (Kitis, 2004). For instance, PAA is being used as a sanitizer in the meat- and poultry-processing plants, where PAA is indicated to be ideal for the clean-in-place systems (Block, 1991; Dychdala, 1988). In medical and pharmaceutical industries, PAA serves as a suitable disinfectant for medical equipment because of its short exposure time and nontoxic decomposition products (Kitis, 2004).

The use of PAA as a disinfectant for municipal wastewater effluents has been drawing more attention in recent years at the laboratory, pilot-scale and full-scale facilities (Gehr et al., 2003; Veschetti et al., 2003; Koivunen and Heinonen-Tanski, 2005; Rossi et al., 2007; Pedersen et al., 2013). Koivunen and Heinonen-Tanski (2005) reported that three log reductions of total coliforms and enterococci in secondary and tertiary effluents could be achieved with 2–7 mg/L PAA and 27 min contact time. A higher PAA dose (10–14 mg/L) was needed to achieve similar levels of inactivation in primary effluents, due to higher amounts of organic matter and suspended solids in the water. Comparatively, PAA is not as effective against viruses. Koivunen and Heinonen-Tanski (2005) found one log of reduction of F-RNA coliphages by 7–15 mg/L PAA and 27 min contact time in primary, secondary and tertiary effluents. Recently, Dunkin et al. (2017) showed that the PAA dose needed for one log reduction in secondary effluent for MS2 bacteriophage and murine norovirus would be around 41.8 mg/L and 2.3 mg/L, respectively, for 30 min of contact time. Apart from the usage in wastewater treatment, PAA has also been used in disinfection for ion exchangers, cooling towers, combined sewer overflow (CSO), stored membrane hollow fibers, and biosolids (Kitis, 2004; Luukkonen and Pehkonen, 2017).

When compared to some of the conventional disinfectants, PAA shows several desirable attributes including stability, safety, quick-reacting and absence of toxic by-products. Among the advantages, not forming mutagenic by-products is especially desirable in drinking water treatment and food processing. Monarca et al. (2002) found that by-products isolated from river water treated with PAA were mostly carboxylic acids with little mutagenicity and no halogen-containing disinfection by-products were observed. However, PAA could have other drawbacks, which may include introduction of organic carbon to the treated effluent.

Although PAA has been used for wastewater disinfection for more than two decades, it has been very limitedly investigated for potential degradation of organic micropollutants such as pharmaceuticals and personal care products (PPCPs) in waters. PPCPs are ubiquitous in the aquatic environment and present a growing concern over their adverse ecological and health effects (Kolpin et al., 2002; Dorne et al., 2007; Santos et al., 2010). Previously, Hey et al. (2012) reported that low doses of PAA were unable to degrade six target pharmaceutical active ingredients in wastewater. The application of PAA in advanced oxidation processes (AOPs) was proposed for organic contaminant destruction (Zhou et al., 2015).

Of the many pharmaceuticals detected in the environment, β-lactam antibiotics, including cephalosporins and penicillins, are among the most prevalent classes. The β-lactam antibiotics have been widely used for more than 80 years, not only to treat human diseases but also in agriculture to prevent infection in plants and livestock (Al-Ahmad et al., 1999; Kummerer, 2001, 2004). Such extensive usage inevitably leads to discharge of these antibiotics into waterways, which could contribute to proliferation of antibiotic-resistant microorganisms (Kummerer, 2004). Various technologies have been investigated for removing residual β-lactam antibiotics from waters. They include photodegradation (Jung et al., 2012) and reactions with oxidants such as chlorine (Acero et al., 2010), chlorine dioxide (Navalon et al., 2008), ozone (Andreozzi et al., 2005; Ikehata et al., 2006; Dodd et al., 2010), ferrate(VI) (Sharma et al., 2013; Karlesa et al., 2014) and AOPs (Arslan-Alaton and Dogruel, 2004; Dail and Mezyk, 2010; Rickman and Mezyk, 2010; Jung et al., 2012; He et al., 2014). To date, the reaction of β-lactams with PAA has not been investigated in detail, and thus is the focus of this study.

As shown in Fig. 1, the structures of cephalosporins and penicillins contain 7-aminodesacetoxy-cephalosporanic acid core moiety and (+)-6-aminopenicillanic acid core moiety, respectively. The electron-rich moieties and functional groups of β-lactams render them likely susceptible to oxidation by PAA.

The objective of this study was to elucidate the reactivity of PAA toward β-lactam antibiotics by determining the reaction kinetics under different pHs, assessing the influence of H_2O_2 on the oxidation reaction, identifying transformation products and reaction pathways, and assessing the reaction kinetics in real water matrices (wastewater and surface water). Four cephalosporins (cefalexin (CFX), cefadroxil (CFR), cefapirin (CFP) and cephalothin (CFT)) and three penicillins (ampicillin (AMP), amoxicillin (AMX) and penicillin G (PG)) were selected for investigation to fully evaluate the impact of structural variation on the oxidation of β-lactams by PAA and facilitate mechanism elucidation.

2. Experimental section

2.1. Chemical reagents

Sodium salts of CFX, CFR, CFP, CFT, AMP, AMX and PG at >98% purity, and commercial peracetic acid solution (~39% PAA, $\leq$6% H_2O_2 and ~45% acetic acid by weight) were purchased from Sigma Aldrich (St. Louis, MO, USA). Hydrogen peroxide (H_2O_2 in water, 30% w/w) was purchased from Fisher Scientific (Waltham, MA, USA). Disodium hydrogen phosphate (Na_2HPO_4), sodium dihydrogen phosphate (NaH_2PO_4) and sodium thiosulfate (NaS_2O_3) were obtained from Sigma-Aldrich. Other employed chemical reagents were obtained from Fisher Scientific or Acros Organics at greater than 99% purity (for solids) or of HPLC grade (for solvents). All reagent solutions were prepared using deionized (DI) reagent water (resistivity >18 Ω M) from a Millipore Mili-Q Ultrapure Gradient A10 purification system. Working solutions of all β-lactams were prepared in DI water at 1.0 mM and stored at 5 °C before use. PAA working solutions were prepared in DI water at 10 g/L. H_2O_2 stock solution was prepared at 11.0 M.

2.2. Surface water and wastewater samples

Grab samples of surface water and wastewater effluent were collected from a municipal drinking water treatment plant and a wastewater treatment plant, respectively, in the Southeast United States. Surface water samples were collected from the reservoir supplying source water to the drinking water treatment plant. Wastewater samples were collected after activated sludge treatment and media filtration and before chlorine disinfection. The water samples were vacuum filtered through 0.5-μm glass-fiber filters immediately upon arrival in the laboratory, stored at 5 °C and used within two days for experiments. Available characteristics of these real water samples are listed below: (1) Surface water sample: pH 6.63, turbidity 3.6 NTU, nitrate 0.23 mg/L as N, nitrite 0.1 μg/L as N, ammonia 0.01 mg/L, phosphate 0.015 mg/L as P, total organic carbon (TOC) 2.1 mg/L, and UV254 absorbance 0.019; (2) Wastewater sample: pH 7.6, chloride ion 58.22 mg/L, phosphate 0.081 mg/L as P, sulfate 44.16 mg/L, TOC 7.33 mg/L, and total inorganic carbon (TIC) 11.76 mg/L.

2.3. Experimental procedures

Batch reactions were conducted in 150-mL amber borosilicate glass bottles with Teflon-lined caps. The solution in the bottle was

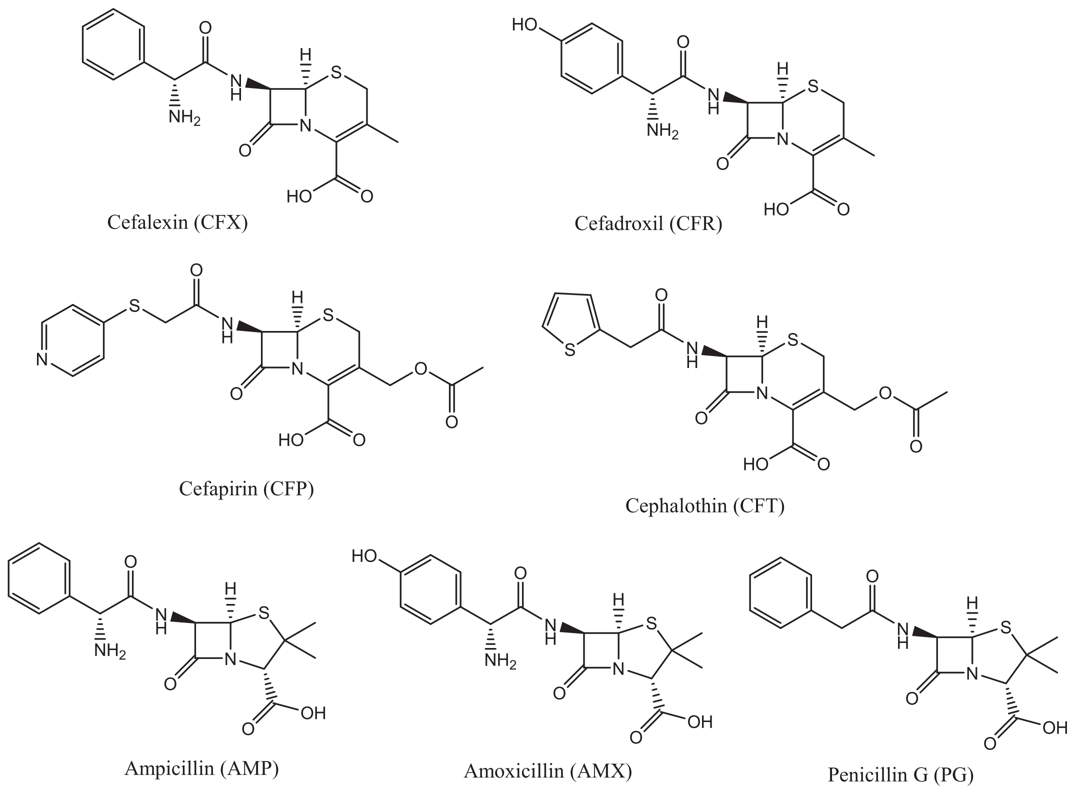

Fig. 1. Structures of β-lactams in this study.

constantly mixed by magnetic stirring at room temperature (25 °C). Phosphate buffer (10 mM) was used to control the solution pH at 5, 7 and 9. Reaction was initiated by adding appropriate volumes of PAA stock to the solution containing buffer and 10 μM β-lactam. The initial concentration of PAA (5–20 mg/L, i.e. 66–263 μM) was in large excess to that of β-lactam. Sample aliquots (1 mL) taken at pre-determined time intervals were immediately quenched by adding 10 μL of 10 mM sodium thiosulfate. The quenched samples were stored in 2-mL amber glass vials at 5 °C and analyzed within 24 h. The same batch experimental procedure was employed in investigating the oxidation of β-lactams by PAA in real water matrices at natural pH without adjustment. The real water samples were confirmed to contain negligible amounts of the target β-lactam antibiotics, and thus the waters were spiked with 10 μM β-lactam prior to addition of PAA.

The reactions with H_2O_2 only were conducted by adding proper volumes of H_2O_2 stock to the solution containing 10 μM β-lactam. The reactions with PAA in the presence of extra H_2O_2 were conducted by adding appropriate volumes of H_2O_2 stock and PAA stock to the solution containing 10 μM β-lactam. The PAA decay experiments were conducted by adding appropriate volumes of PAA to DI water and real water samples (initial PAA concentration was 10 mg/L). All the experiments were conducted in at least duplicate or more.

2.4. Analytical methods

The PAA stock solution, including 39% PAA and 6% H_2O_2, was regularly calibrated by using titration methods. The combined concentration of PAA and H_2O_2 was first measured with the indirect iodometric titration, by adding potassium iodide and ammonium molybdate (as a catalyst) to produce the liberated iodine and then titrating the iodine with sodium thiosulfate. Then, the concentration of H_2O_2 in PAA solution or in pure H_2O_2 stock solution was titrated with potassium permanganate under acidic pH. The PAA concentration in stock solution could be obtained by subtracting H_2O_2 concentration from the combined concentration of PAA and H_2O_2.

The PAA working solution at 10 g/L was prepared weekly based on the concentration of PAA stock solution determined by the above method through appropriate dilution and stored at 5 °C. The residual PAA concentrations in experiments were quantified by the standard *N,N*-diethyl-*p*-phenylenediamine ferrous ammonium sulfate (DPD-FAS) titration method (APHA et al., 2005).

All β-lactams were analyzed by an Agilent 1100 high performance liquid chromatography (HPLC) equipped with a diode-array UV–visible detector. Sample injection of 20 μL was separated on a Zorbax RX-C18 column (4.6 × 250 mm, 5 μm) at the flow rate of 0.3 mL/min. Isocratic elution was employed by 0.1% formic acid in water (A) and pure methanol (B) at specific volume ratio (80:20 v/v for CFX, AMX, CFP and CFR; 70:30 v/v for CFT and AMP; 60:40 v/v for PG). The detection wavelength was 220 nm.

Transformation products were analyzed by an Agilent 1100 HPLC/UV/MSD system with a Zorbax SB-C18 column (2.4 × 150 mm, 5 μm). Gradient elution was carried out using 0.1% formic acid in water (A) and pure methanol (B) at a flow rate of 0.3 mL/min. The ratios of A and B were 90:10 v/v (AMX), 80:20 v/v (CFX, CFP and CFR), 70:30 v/v (AMP) and 60:40 v/v (CFT and PG). The injection volume was 20 μL. The products were analyzed by electrospray ionization at positive mode (ESI+) at the fragmentation voltage 70–220 eV with a mass scan range of m/z 50–500. Other parameters were set as follows: drying gas 6 L/min at 350 °C, capillary voltage 4000 V, and nebulizer pressure 25 psig.

2.5. Computational method

All the computations were performed using Gaussian 03 (Frisch et al., 2003). Geometry optimization was executed without any constraints using the B3LYP method with 6-31G(d,p) basis set in the gas phase.

3. Results and discussion

3.1. Reaction kinetics of β-lactams with PAA

For all the β-lactams investigated for reaction with PAA, the plots of ln([β-lactam]/[β-lactam]$_0$) versus time showed good linearity (Supplementary Information (SI) Fig. S1), suggesting that the reaction was first order with respect to β-lactams. The first-order reaction with respect to PAA was confirmed by reacting 10 μM of β-lactam with various doses (5, 10, 15, and 20 mg/L, i.e., 66–263 μM) of PAA at pH 7. The excess condition of PAA was confirmed by monitoring the residual PAA concentration; for example, at the dose of 10 mg/L (i.e., 131 μM) PAA, the residual PAA concentration was found to be 105–125 μM after 30 min of reaction time with various β-lactams. For each reaction, a linear relationship was found between the first-order rate constant k_{obs} for the loss of parent β-lactam and the initial PAA concentration (SI Fig. S2). Thus, the reaction between β-lactams and PAA can be described by a second-order rate expression:

$$\frac{d[\beta-\text{lactam}]}{dt} = -k_{\text{app}}[\beta-\text{lactam}][\text{PAA}] \quad (3)$$

where k_{app} is the apparent second-order rate constant for the overall reaction, and [β-lactam] and [PAA] are the concentrations of total β-lactam and total PAA, respectively. The values of k_{app} were obtained from the slopes of lines in Fig. S2. Among the β-lactams tested, the reactivity to PAA (based on k_{app} shown in Table 1) followed the order of CFR ~ CFX > AMP ~ AMX > CFT ~ CFP ~ PG. The above trend agrees with some of the trends reported for the reactions of β-lactams with other oxidants qualitatively. For example, Dodd et al. (2006) found that PG (4.8×10^3 $M^{-1}s^{-1}$) reacted more slowly than CFX (8.7×10^4 $M^{-1}s^{-1}$) to ozone. Karlesa et al. (2014) found PG (114 $M^{-1}s^{-1}$) much less reactive than AMP (418 $M^{-1}s^{-1}$) and AMX (771 $M^{-1}s^{-1}$) to Fe(VI). Navalon et al. (2008) reported that PG reacted much more slowly than AMX and CFR to chlorine dioxide, although the rate constants were not determined. The obvious difference in k_{app} values among various β-lactams to PAA is likely caused by different β-lactam ring moieties and peripheral functional groups, which will be discussed later based on reactive sites and product identification.

It is interesting to compare the reaction rates of β-lactams with PAA to those reported with other oxidants commonly used in water and wastewater treatment. The second-order rate constants (at pH 7) of penicillins with ferrate(VI) range from 110 to 770 $M^{-1}s^{-1}$ (Karlesa et al., 2014). The second-order rate constants (at pH 7) of β-lactams with ozone are at 10^3-10^6 $M^{-1}s^{-1}$ (Andreozzi et al., 2005; Dodd et al., 2006). The second-order rate constant of AMX with aqueous chlorine is 1.19×10^5 $M^{-1}s^{-1}$ at pH 7 (Acero et al., 2010). Evidently, the β-lactams react with PAA (Table 1) considerably more slowly than with the other oxidants. Thus, PAA's reactivity to β-lactams is modest, despite the relatively high oxidation potential of PAA. When AOPs were used in the oxidation, the reaction rate constants of β-lactams with radical species such as •OH and $SO_4^{\bullet -}$ were even higher at $k_{OH} \approx k_{SO_4} \approx 10^9$ $M^{-1}s^{-1}$ (Sharma et al., 2013). It has been suggested that the disinfectant activity of PAA may be related to release of reactive oxygen species through decomposition of PAA (Liberti and Notarnicola., 1999; Flores et al., 2013). However, on the basis of the relatively small rate constants of β-lactams with PAA observed in this study (Table 1), involvement of radical species was unlikely. Rather, the β-lactams were oxidized by PAA as an oxidant. Although PAA has a slower reaction rate to the antibiotics than other oxidants, PAA has the advantage of not producing harmful chlorinated disinfection by-products such as trihalomethanes (THMs), a problem shown in chlorine oxidation of antibiotics (Acero et al., 2010).

Table 1
Second-order rate constants of β-lactam antibiotics with PAA at pH 7 and 25 °C.

Compound	k_{app} ($M^{-1}s^{-1}$)
Cefalexin (CFX)	41.43 ± 1.69
Cefadroxil (CFR)	44.38 ± 0.96
Cephalothin (CFT)	17.77 ± 0.48
Cefapirin (CFP)	15.56 ± 0.29
Penicillin G (PG)	19.04 ± 0.37
Ampicillin (AMP)	28.77 ± 1.13
Amoxicillin (AMX)	28.24 ± 1.11

3.2. Effect of H_2O_2 on oxidation of β-lactams by PAA

Because H_2O_2 was present in the commercial PAA solution as mentioned above (Eq. (1)), the impact of H_2O_2 needed to be evaluated. As a strong oxidant, H_2O_2 may contribute to oxidation of antibiotics. To investigate the influence of H_2O_2 on the reactions, four β-lactams (CFX, CFT, PG and AMP) were reacted with 33 μM H_2O_2 only (similar to the concentration of H_2O_2 measured in the reaction solution of PAA, in which the PAA concentration was 131 μM). Results (SI Fig. S3) showed little degradation of β-lactams by H_2O_2 after 1-h reaction time at either pH 5 or 7. Similar results were obtained at even higher H_2O_2 doses of 330 and 3300 μM (data not shown), which demonstrated that H_2O_2 had very weak oxidizing capacity toward β-lactams. Further experiments were conducted by adding extra H_2O_2 (330 μM and 3300 μM) to the PAA reaction solution with β-lactams. There was no obvious increase in the degradation rate of β-lactams with the presence of extra H_2O_2 compared to those without (SI Table S1). The above experiments confirmed that it was PAA, not H_2O_2, that dominated the oxidation reaction of β-lactams. In analogy, by varying the proportion of PAA to H_2O_2, Lubello et al. (2002) determined that it was PAA, not H_2O_2, that was responsible for the biocidal action. Even though the oxidation targets were different in this study and the study by Lubello et al. (2002), both studies showed PAA as the key oxidant in the PAA/H_2O_2 mixture.

3.3. Effect of pH on oxidation of β-lactams by PAA

To investigate the effect of pH on the reaction of β-lactams with PAA, 10 μM of antibiotics were reacted with 131 μM of PAA at pH 5, 7 and 9, respectively. Results showed that the rate constants at pH 5 and pH 7 were comparable, but decreased by about an order of magnitude at pH 9 for each tested β-lactam (Fig. 2).

The speciation of PAAH and PAA^- varies at different pH due to acid-base dissociation reaction of PAA (Eq. (2)). Solution pH may also affect the stability of PAA. It is known from the literature that spontaneous decomposition (Eq. (4)) and hydrolysis (Eq. (5)) are potential reactions of PAA in aqueous solution without metal ions (Yuan et al., 1997a,b). In spontaneous decomposition (Eq. (4)), PAA is decomposed to form acetic acid and O_2, and the reaction is proposed to occur via nucleophilic attack of a PAA^- anion on a PAAH molecule. The reaction rate of spontaneous decomposition reaches a maximum at around pH 8.2 (pKa of PAA) and was slower at either lower or higher pH (Yuan et al., 1997a). In hydrolysis (Eq.

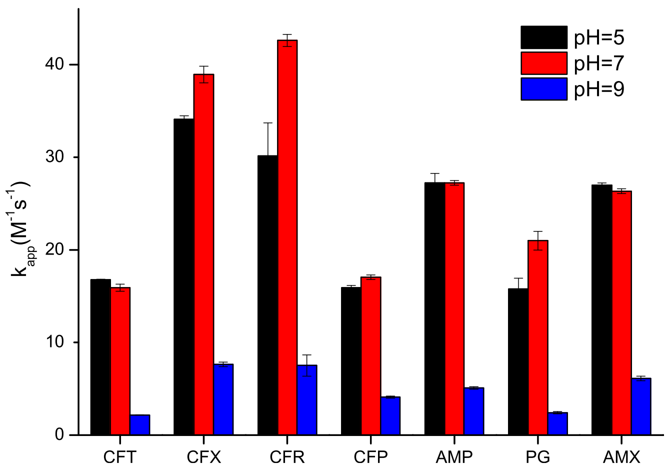

Fig. 2. The apparent second-order rate constants of β-lactams with PAA at different pH ($[\beta\text{-lactam}]_0 = 10\ \mu M$, $[PAA]_0 = 131\ \mu M$).

(5)), PAA reacts with OH^- to form acetic acid and H_2O_2, and the reaction rate increases as pH increases (Yuan et al., 1997b). The reaction kinetics of spontaneous decomposition and hydrolysis were investigated in detail by Yuan et al. (1997a,b) and are represented by the rate equation (Eq. (6)) that combines both reactions for the loss of total PAA in aqueous solution at different pH and temperature.

$$2\ CH_3C(=O)OOH \rightarrow 2\ CH_3C(=O)OH + O_2 \tag{4}$$

$$CH_3C(=O)OOH + H_2O \xrightarrow{OH^-} CH_3C(=O)OH + H_2O_2 \tag{5}$$

$$-\frac{d[PAA]_{total}}{dt} = 9.21 \times 10^{13} \cdot e^{-\frac{11338.71}{T}} \cdot \frac{2[H^+]/K_a}{\left(1+[H^+]/K_a\right)^2} \cdot \left([PAA]_{total}\right)^2 + \left(2.32 \times 10^8 \cdot e^{-\frac{7488.68}{T}} \cdot \frac{K_a}{[H^+]+K_a} + 1.19 \times 10^9 \cdot e^{-\frac{5903.40}{T}} \cdot \frac{[H^+]}{[H^+]+K_a}\right)\left[OH^-\right][PAA]_{total} \tag{6}$$

Using the kinetic model by Yuan et al. (1997a,b), the reaction rate constants of PAA for Eq. (4) and Eq. (5) were calculated according to the experimental conditions of this study (SI Table S2). Based on these rate constants, it was determined that the spontaneous decomposition and hydrolysis of PAA were negligible at pH 5 and 7. At pH 9, the combination of both reactions yielded only 0.76% loss of PAA after 30 min of reaction time. Although spontaneous decomposition of PAA may occur via a radical pathway (e.g., in the presence of metal ions (Yuan et al., 1997b)), radical reactions are negligible in this study due to absence of metal ions and the results discussed in Section 3.1. Thus, it can be concluded that pH primarily influenced the dissociation of PAA. As Fig. S4 shows, neutral PAAH is dominant (over 94%) at pH < 7, while anionic PAA^- species becomes dominant (over 85%) at pH > 9. When solution pH was 5 and 7, PAAH was the major species, which exhibited stronger oxidizing power toward antibiotics. The similar second-order rate constants (except CFX, CFR and PG) at pH 5 and 7 were resulted from the same concentration of PAAH existing in the solution. In contrast, when solution pH was 9, PAA^- became dominant. Thus, less PAAH led to a lower value of k_{app}.

Solution pH also affects the speciation of β-lactams. Acidity constants are associated with β-lactams' carboxylic acid group (pKa = 2.69–3.63), phenylglycinyl amino group (pKa = 7.22–9.63) and phenol group (pKa = 9.48–9.63) if present (Fig. 1 and SI Table S3). The carboxylic acid group is deprotonated for all the β-lactams at pH 5–9, and the observed pH trend in Fig. 2 does not correspond to the pKa values of the β-lactams specifically. As will be discussed in the next section, β-lactams' sulfur group was identified to be the main reactive site to PAA and does not change speciation at pH 5–9. Thus, the β-lactams' speciation in the investigated pH range was not an important factor in the impact of pH on the reaction rate.

3.4. Evaluation of reaction moieties, products and pathways

As Table 1 shows, CFR (44.38 $M^{-1}s^{-1}$) and CFX (41.43 $M^{-1}s^{-1}$) were most reactive to PAA among the β-lactams, followed by AMP (28.77 $M^{-1}s^{-1}$) and AMX (28.24 $M^{-1}s^{-1}$), and then PG (19.04 $M^{-1}s^{-1}$), CFT (17.77 $M^{-1}s^{-1}$) and CFP (15.56 $M^{-1}s^{-1}$). The difference in reactivity is likely related to compound structures. There are two major structural differences among these β-lactams: (1) a six-membered dihydrothiazine ring (cephalosporins) vs. a five-membered thiazolidine ring (penicillins) fused to the β-lactam ring; and (2) the presence or absence of a phenylglycinyl amino group on the side chain.

In the oxidation of organic substrates by PAA, PAA is expected to seek atoms/moieties with available electrons. The thioether sulfur in the β-lactams is an electronic-rich site and is present in all the β-lactams investigated. Literature has indicated disruption of −SH and −S−S− bonds within enzymes and cell walls by PAA (Kitis, 2004). Previous research reported formation of sulfoxide (M+16) products after ozone oxidation of β-lactams (Dodd et al., 2010), and formation of sulfoxide and sulfone (M+32) products after ferrate(VI) oxidation of β-lactams (Karlesa et al., 2014), where M represents the parent compound molecular weight. However, results in Table 1 indicate that β-lactams with the same thioether group do not necessarily exhibit the same reactivity to PAA. Particularly, β-lactams that contain the phenylglycinyl amino group all exhibited a higher rate constant than those without, i.e., CFR/CFX vs. CFT/CFP, and AMP/AMX vs. PG (Fig. 1 and Table 1). Hence, the phenylglycine amino group appears to play a critical role as well. In contrast, results in Table 1 revealed that PAA is probably not reactive to a phenolic structure, demonstrated by the similar rate constants of CFX vs. CFR and AMP vs. AMX (Fig. 1 and Table 1).

We hypothesize that β-lactams receive electrophilic attack by PAA and lose electrons in the oxidation reaction. To further understand the effects of β-lactams' functional groups on the reaction rate, density functional theory (DFT) calculations were conducted to evaluate the nucleophilicity of various β-lactams. The global nucleophilicity with the highest occupied molecular orbital (HOMO) energy was used to describe the nucleophilicity N index, namely

$$N = E_{HOMO(Nu)}(eV) - E_{HOMO(TCE)}(eV) \tag{7}$$

where tetracyanoethylene (TCE) was taken as a reference because it has the lowest HOMO energy in a series of molecules, giving a positive nucleophilicity value for various β-lactams (SI Tables S4–S13).

Fig. 3 shows that a reasonably good positive correlation exists between the global nucleophilicity of β-lactams and the reaction rate constant with PAA. This result supports that the attack of β-lactams by PAA is highly electrophilic in nature. This finding is consistent with the reactants' structures, as the peroxyl group of

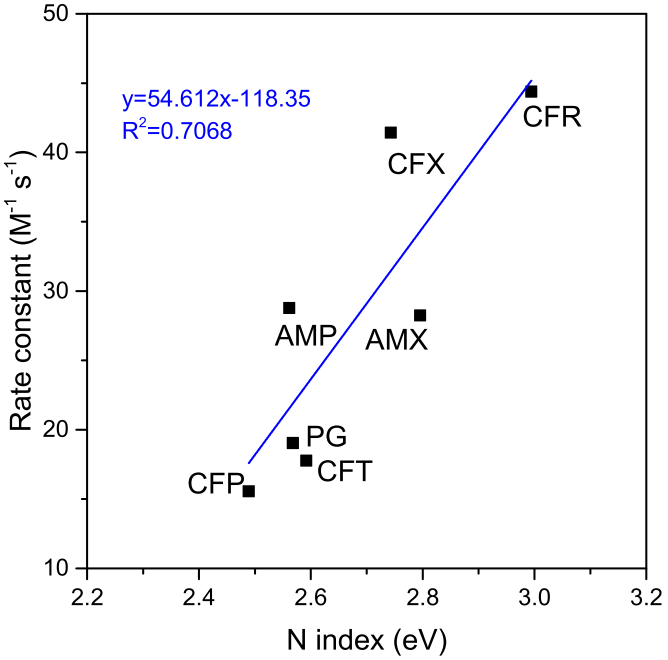

Fig. 3. Correlation between the nucleophilicity N index (eV) and the rate constant (M^{-1} s^{-1}) to PAA of seven different β-lactams.

PAA is known to be electron-deficient (Chipiso et al., 2016), while the S atom and amino group on β-lactams are generally electron-rich sites.

Three β-lactams (CFX, AMP and PG) and a hypothetical model compound CFXN (CFX without the phenylglycinyl $-NH_2$ group) were selected to further study the role of functional groups by frontier orbital analysis. The HOMO location generally means the sites most likely to be oxidized and lose electrons. Fig. 4 shows that the HOMOs are mainly located at the five-membered ring of PG, the phenylglycine moiety of AMP, and the six-membered ring of CFX and CFXN, respectively. This suggests that the S-containing ring and phenylglycinyl amino group of β-lactams are both potential reactive sites for oxidation by PAA.

For β-lactams that do not have the phenylglycinyl amino group, there was little difference in the k_{app} with PAA between the five- and six-membered S-containing rings (e.g., PG ~ CFP ~ CFT, Table 1). The presence of the phenylglycinyl amino group increases the k_{app} with PAA, and the enhancement effect is more pronounced in β-lactams with a six-membered ring than those with a five-membered ring. For example, the k_{app} of CFX and CFR with PAA are about 2.6 times of those of CFP and CFT, while the k_{app} of AMX and AMP with PAA are about 1.5 times of that of PG (Table 1). This trend may be explained by the HOMO location analysis. As shown by PG vs. AMP in Fig. 4, the HOMO location shifts from the five-membered ring to the phenylglycinyl amino group when present, which may facilitate PAA attack toward this site. In contrast, for CFXN and CFX, the HOMO location remains at the six-membered S-containing ring regardless of the presence of the phenylglycinyl amino group; instead, the presence of the amino group increases the HOMO energy at the six-membered ring (Fig. 4). Thus, we propose that the six-membered ring of β-lactams can be "activated" by the side-chain phenylglycinyl amino group, with electron redistribution on the lactam molecule that renders the six-membered S-containing ring more reactive than the amino group to PAA.

Oxidation products analysis was also conducted to help understand the different reactivity of β-lactams to PAA. Oxidation products of 10 μM β-lactams by 131 μM PAA at pH 7 (similar to the reaction conditions for k_{app} determination) after reaction time of 5 min and 2 h were analyzed by LC/MS. The LC/MS chromatograms and spectra of AMP are provided in the SI Figs. S5–S7. At the beginning of the reaction, the only peak with m/z of 350 ($M + H^+$) detected at retention time (RT) of 3.573 min was AMP (SI Fig. S5). After reaction time of 5 min, a new peak with m/z of 366 ($M{+}16 + H^+$) at RT 2.696 min, in addition to the AMP peak, was detected (SI Fig. S6). After 2 h of reaction time, the m/z 366 product peak grew to a prominent peak (RT = 2.956 min) while the parent AMP was no longer detected (SI Fig. S7), and no other significant product peaks were found. The other β-lactams exhibited the same product formation patterns as AMP with generation of a M+16 product only (data not shown).

The very similar product formation patterns among various β-lactams strongly imply that they may follow the same reaction mechanism. The oxidation product is likely the sulfoxide of β-lactam (Fig. 5). Two stereoisomeric ((*R*)- and (*S*)-) sulfoxide products of PG with exactly the same MS spectra but different retention times were detected by Dodd et al. (2010) in the ozonation of PG. In comparison, the sulfoxide products were found as one mixture by LC/MS in this study, but matched the study of Dodd et al. (2010) in terms of exhibiting the correct m/z ratio and a shorter retention time than the parent β-lactam. Furthermore, other findings of this study and the literature also support the proposed product

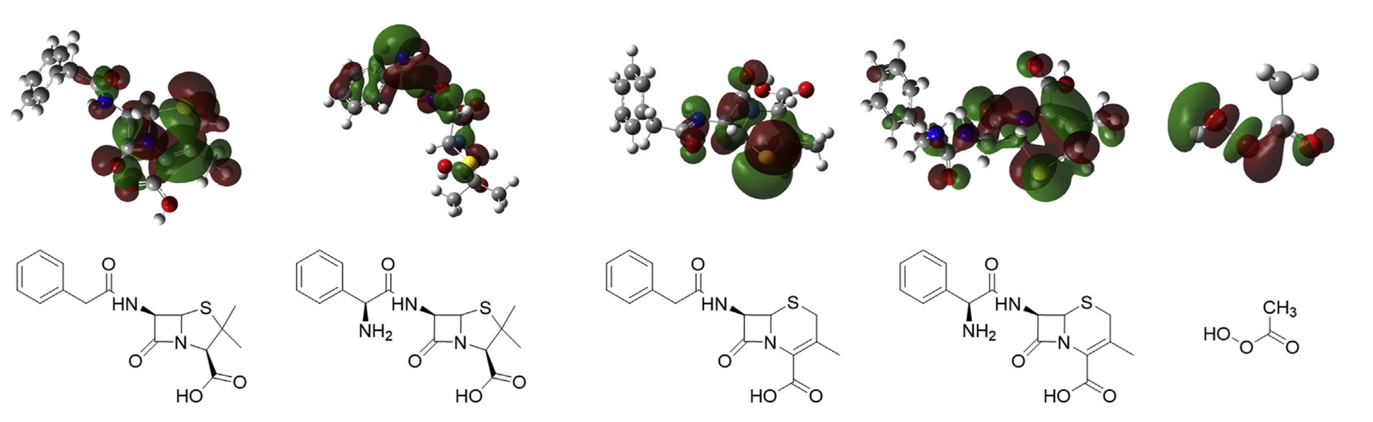

Fig. 4. HOMO MOs in optimized geometry of PG, AMP, CFXN and CFX, and LUMO in PAA.

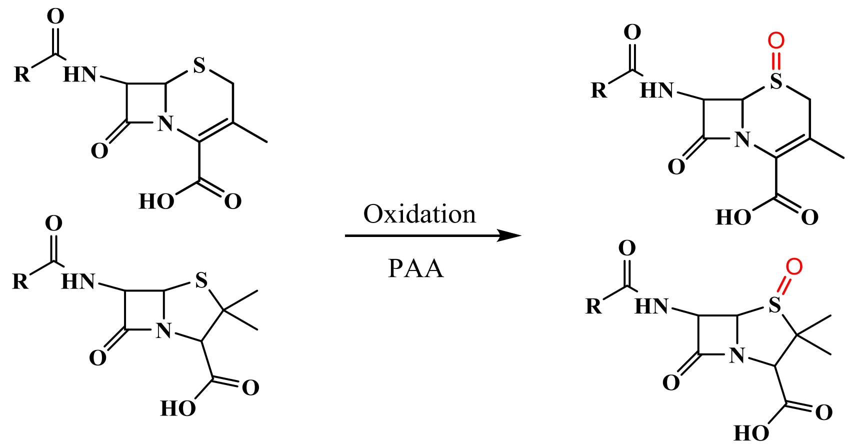

Fig. 5. Oxidation of β-lactams by PAA to generate sulfoxide products.

formation. First, PAA was found in other experiments to have low reactivity to compounds (including amino acids and pharmaceuticals) that contain amine functional groups but significant reactivity to compounds with sulfur-containing groups (Chipiso et al., 2016; Kerkaert et al., 2011). Second, if PAA oxidized the phenylglycinyl amino group of β-lactams, such oxidation would likely generate an iminium intermediate which would decompose quickly in water to yield breakdown products (Chen et al., 2016). This reaction path is unlikely because products from bond scission of β-lactams were not found in the experiments. Third, PAA is a weaker oxidant compared to others such as ferrate(VI), and relatively mild experimental conditions (10 mg/L PAA and 2 h reaction time) well within wastewater treatment conditions were employed in this study. Thus, even though Karlesa et al. (2014) reported Fe(VI) oxidation of CFX's phenylglycinyl amino group and generation of ammonium ion product, PAA as a weaker oxidant exhibited limited ability to oxidize β-lactams' phenylglycinyl amino group. Also, in contrast to Fe(VI), PAA converted the thioether sulfur to a sulfoxide (M+16) but could not further oxidize sulfoxide to sulfone (M+32).

Overall, on the basis of the evidence discussed above, it can be concluded that the thioether sulfur of β-lactams is the main reactive site to PAA and is oxidized to sulfoxide. Presence of the phenylglycinyl amino group can significantly influence electron distribution and HOMO location and energy on β-lactams in ways that enhance the apparent reactivity to PAA. According to the literature, the sulfoxide product of PG contained less than 15% of activity as PG toward bacteria while such product of CFX retained ~83% antibacterial activity compared to CFX (Dodd et al., 2010). Thus, the transformation products of β-lactams by PAA likely have lost some antibacterial activity but the extent may vary with different β-lactams. More research should be conducted to evaluate the toxicological effects of the transformation products of β-lactams by PAA to fully assess the adequacy of this oxidation treatment.

3.5. Reactions in environmental water matrices

Oxidation of β-lactams by PAA was also conducted in real water samples to investigate the impact of real water matrices on the reaction kinetics. A wastewater and a surface water samples were spiked with 10 μM of antibiotics (CFR, CFX, AMP, AMO, CFT, CFP, and PG) individually, followed by addition of 10 mg/L (i.e., 131 μM) of PAA. Both real water samples contained relatively low concentrations of inorganic nitrogen and exhibited modest consumption of

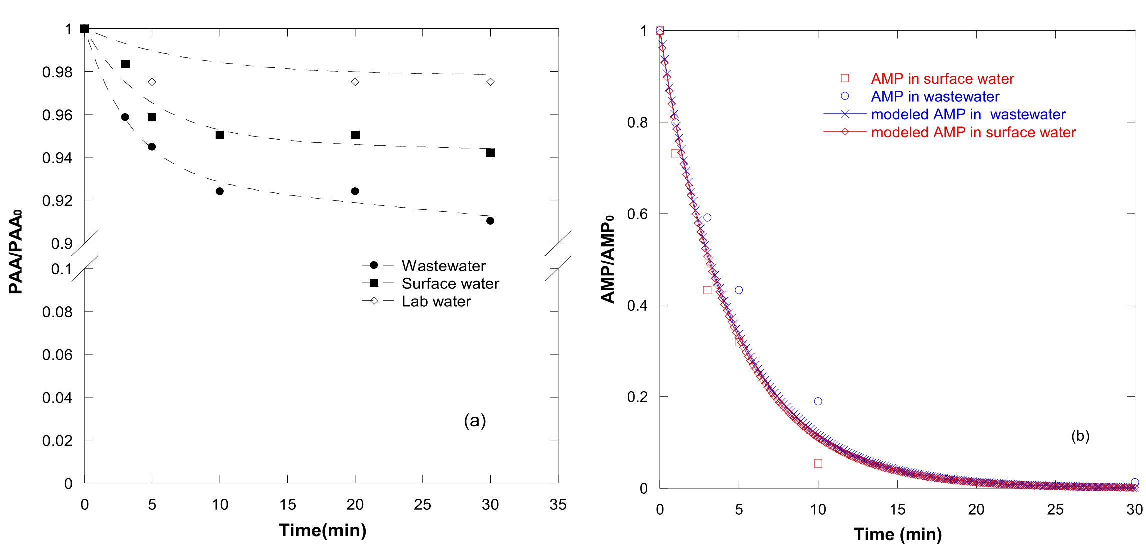

Fig. 6. (a) Decay of PAA in real water samples ($[PAA]_0 = 131$ μM, pH = 6.63 (surface water) or 7.6 (wastewater)); (b) Decay of AMP in real water samples by PAA ($[PAA]_0 = 131$ μM, $[AMP]_0 = 10$ μM).

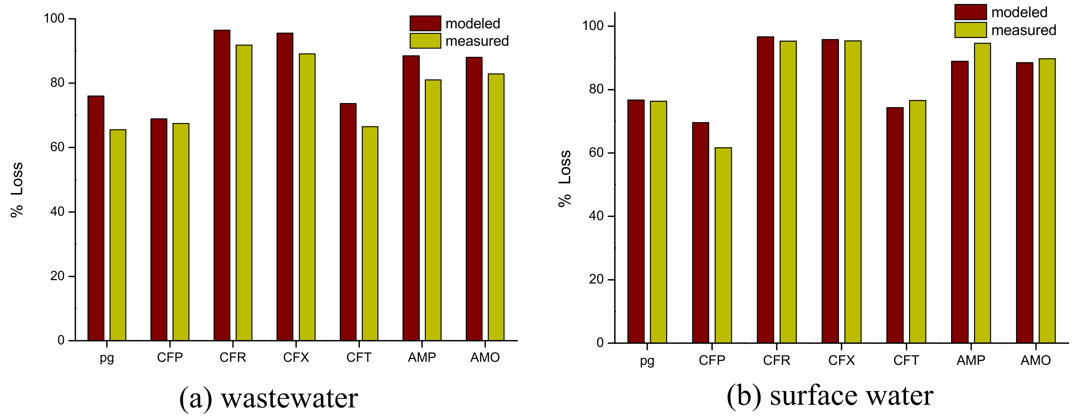

Fig. 7. Modeled and measured losses of β-lactams in two real water samples ((a) wastewater; and (b) surface water). $[PAA]_0 = 10$ mg/L, contact time = 10 min, wastewater pH = 7.6, and surface water pH = 6.63.

PAA (Fig. 6a). The decay of PAA in the real water samples could be attributed to reactions with two different groups of substrates, which had high and low reactivities with PAA, respectively, and was modeled by Equation (8):

$$[\mathrm{PAA}]_t = [\mathrm{PAA}]_{t0}\left[\alpha e^{-k_1 t} + (1-\alpha)e^{-k_2 t}\right] \tag{8}$$

where $[\mathrm{PAA}]_t$ and $[\mathrm{PAA}]_{t0}$ represent PAA concentration at time t and initially, respectively; α represents the percentage of highly reactive substrates; k_1 and k_2 represent the pseudo-first-order rate constants for highly reactive and slowly reactive substrates, respectively, with PAA. The decay of PAA in lab water and real water samples were fitted by Eq. (8) (Fig. 6a).

Since the reaction of antibiotics and PAA followed the second-order kinetics (Eq. (3)), incorporation of Eq. (8) into Eq. (3) and integration lead to Eq. (9):

$$[\beta-\mathrm{lactam}] = [\beta-\mathrm{lactam}]_0 e^{\left\{-k_{app}[\mathrm{PAA}]_0 \int_0^t \left[\alpha e^{-k_1 t} + (1-\alpha)e^{-k_2 t}\right] dt\right\}} \tag{9}$$

where k_{app} is the apparent second-order rate constant of specific β-lactam determined in reagent water as shown in Table 1. Fig. 6b shows the expected and measured decay of AMP, as an example, in the two real water matrices. The model agreed well with the experimental data for surface water, and slightly overestimated the decay rate of AMP in wastewater.

Fig. 7 depicts the expected (based on Eq. (9)) and measured losses of all the tested β-lactam antibiotics in the two real water matrices under PAA dosage of 10 mg/L and 10 min of contact time. The results suggested that decay of the β-lactams at 62–95% could be expected, depending on the water matrices. As shown in Fig. 7a, for each β-lactam, the model slightly overestimated the rate of antibiotic decay in the wastewater matrix. A definitive reason for this overestimation is not available and needs further research to evaluate the impacts of different constituents in wastewaters on PAA decay and β-lactam degradation by PAA. As for the decay in surface water matrix (Fig. 7b), little difference existed between the modeled and measured losses of antibiotics, indicating that the degradation of β-lactams by PAA can be accurately predicted in relatively clean surface water. Overall, the trends of percentage loss of β-lactams by PAA oxidation in real water matrices were consistent with those observed in reagent water matrix (Section 3.1), i.e., a higher k_{app} contributed to a higher loss and vice versa.

4. Conclusions

This study is among the first to investigate the reactions of a wide range of β-lactams with PAA, and provides the following new knowledge regarding oxidation of β-lactams by PAA:

(1) The β-lactams react rapidly with PAA and H_2O_2 has negligible effect on the reaction. Oxidation of β-lactams by PAA is much faster at pH 5 and 7 than at pH 9.
(2) The thioether sulfur of β-lactams is oxidized to sulfoxide by PAA. While the phenylglycinyl amino group in some β-lactams is difficult to be oxidized by PAA, it can significantly influence the apparent reactivity of β-lactams to PAA by changing electron distribution and the HOMO energy.
(3) The reaction rate constants obtained in clean water matrix can be used to accurately model the decay of β-lactams by PAA in surface water sample matrix, and only slightly overestimate the decay in wastewater matrix.

Acknowledgements

The support for Dr. Kejia Zhang for study at Georgia Tech and for this study was from the National Research Council of Science and Technology Major Project of China (Water Pollution Control and Treatment) (No. 2012ZX07403-003), Natural Science Foundation of Zhejiang Province (No. LY17E080014), the Fundamental Research Funds for the Central Universities (No. 2016FZA4017). This study was also partially supported by the U.S. National Science Foundation grant CHE-1609361.

Appendix A. Supplementary data

Supplementary data related to this article can be found at http://dx.doi.org/10.1016/j.watres.2017.06.057.

References

Acero, J.L., Benitez, F.J., Real, F.J., Roldan, G., 2010. Kinetics of aqueous chlorination of some pharmaceuticals and their elimination from water matrices. Water Res. 44 (14), 4158–4170.
Al-Ahmad, A., Daschner, F.D., Kummerer, K., 1999. Biodegradability of cefotiam, ciprofloxacin, meropenem, penicillin G, and sulfamethoxazole and inhibition of wastewater bacteria. Arch. Environ. Contam. Toxicol. 37 (2), 158–163.
Andreozzi, R., Canterino, M., Marotta, R., Paxeus, N., 2005. Antibiotic removal from wastewaters: the ozonation of amoxicillin. J. Hazard. Mater. 122 (3), 243–250.
APHA, AWWA, WEF, 2005. Standard Methods for the Examination of Water and Wastewater, twenty-first ed. Washington, D.C, USA.
Arslan-Alaton, I., Dogruel, S., 2004. Pre-treatment of penicillin formulation effluent

by advanced oxidation processes. J. Hazard. Mater. 112 (1), 105–113.
Awad, M.I., Denggerile, A., Ohsaka, T., 2004. Electroreduction of peroxyacetic acid at gold electrode in aqueous media. J. Electrochem. Soc. 151 (12), E358–E363.
Block, S.S., 1991. Peroxygen compounds. In: Block editor, S.S. (Ed.), Disinfection, Sterilization, and Preservation, fifth ed. Lippincott Williams & Wilkins, Philadelphia, PA, pp. 185–204 (Chapter 9).
Chen, J., Sun, P., Zhang, Y., Huang, C.-H., 2016. Multiple roles of Cu(II) in catalyzing hydrolysis and oxidation of β-lactam antibiotics. Environ. Sci. Technol. 50 (22), 12156–12165.
Chipiso, K., Logan, I.E., Eskew, M.W., Omondi, B., Simoyi, R.H., 2016. Kinetics and mechanism of bioactivation via S-oxygenation of anti-tubercular agent ethionamide by peracetic acid. J. Phys. Chem. A 120 (41), 8056–8064.
Dail, M.K., Mezyk, S.P., 2010. Hydroxyl-radical-induced degradative oxidation of beta-lactam antibiotics in water: absolute rate constant measurements. J. Phys. Chem. A 114 (32), 8391–8395.
Dodd, M.C., Buffle, M.-O., von Gunten, U., 2006. Oxidation of antibacterial molecules by aqueous ozone: moiety-specific reaction kinetics and application to ozone-based wastewater treatment. Environ. Sci. Technol. 40, 1969–1977.
Dodd, M.C., Rentsch, D., Singer, H.P., Kohler, H.-P.E., von Gunten, U., 2010. Transformation of β-lactam antibacterial agents during aqueous ozonation: reaction pathways and quantitative bioassays of biologically-active oxidation products. Environ. Sci. Technol. 44, 5940–5948.
Dorne, J.L., Ragas, A.M.J., Frampton, G.K., Spurgeon, D.S., Lewis, D.F., 2007. Trends in human risk assessment of pharmaceuticals. Anal. Bioanal. Chem. 387 (4), 1167–1172.
Dunkin, N., Weng, S.C., Schwab, K.J., McQuarrie, J., Bell, K.Y., Jacangelo, J.G., 2017. Comparative inactivation of murine norovirus and MS2 bacteriophage by peracetic acid and monochloramine in municipal secondary wastewater effluent. Environ. Sci. Technol. 51 (5), 2972–2981.
Dychdala, G.R., 1988. New hydrogen peroxide-peroxyacetic acid disinfectant.In: Proceedings of the 4th Conference on Progresses in Chemical Disinfection, Binghamton, NY, 315–342.
Flores, M.J., Lescano, M.R., Brandi, R.J., Cassano, A.E., Labas, M.D., 2013. A novel approach to explain the inactivation mechanism of Escherichia coli employing a commercially available peracetic acid. Water Sci. Technol. 69, 358–363.
Frisch, M.J., Trucks, G.W., Schlegel, H.B., Scuseria, G.E., Robb, M.A., Cheeseman, J.R., Montgomery, J.A., Vreven, T., Kudin, K.N., Burant, J.C., Millam, J.M., Iyengar, S.S., Tomasi, J., Barone, V., Mennucci, B., Cossi, M., Scalmani, G., Rega, N., Petersson, G.A., Nakatsuji, H., Hada, M., Ehara, M., Toyota, K., Fukuda, R., Hasegawa, J., Ishida, M., Nakajima, T., Honda, Y., Kitao, O., Nakai, H., Klene, M., Li, X., Knox, J.E., Hratchian, H.P., Cross, J.B., Bakken, V., Adamo, C., Jaramillo, J., Gomperts, R., Stratmann, R.E., Yazyev, O., Austin, A.J., Cammi, R., Pomelli, C., Ochterski, J.W., Ayala, P.Y., Morokuma, K., Voth, G.A., Salvador, P., Dannenberg, J.J., Zakrzewski, V.G., Dapprich, S., Daniels, A.D., Strain, M.C., Farkas, O., Malick, D.K., Rabuck, A.D., Raghavachari, K., Foresman, J.B., Ortiz, J.V., Cui, Q., Baboul, A.G., Clifford, S., Cioslowski, J., Stefanov, B.B., Liu, G., Liashenko, A., Piskorz, P., Komaromi, I., Martin, R.L., Fox, D.J., Keith, T., Laham, A., Peng, C.Y., Nanayakkara, A., Challacombe, M., Gill, P.M.W., Johnson, B., Chen, W., Wong, M.W., Gonzalez, C., Pople, J.A., 2003. Gaussian 03, Revision c.02.
Gehr, R., Wagner, M., Veerasubramanian, P., Payment, P., 2003. Disinfection efficiency of peracetic acid, UV and ozone after enhanced primary treatment of municipal wastewater. Water Res. 37 (19), 4573–4586.
He, X., Mezyk, S.P., Michael, I., Fatta-Kassinos, D., Dionysiou, D.D., 2014. Degradation kinetics and mechanism of β-lactam antibiotics by the activation of H_2O_2 and $Na_2S_2O_8$ under UV-254nm irradiation. J. Hazard. Mater. 279, 375–383.
Hey, G., Ledin, A., Jansen, J.L.C., Andersen, H.R., 2012. Removal of pharmaceuticals in biologically treated wastewater by chlorine dioxide or peracetic acid. Environ. Technol. 33, 1041–1047.
Ikehata, K., Naghashkar, N.J., Ei-Din, M.G., 2006. Degradation of aqueous pharmaceuticals by ozonation and advanced oxidation processes: a review. Ozone Sci. Eng. 28 (6), 353–414.
Jung, Y.J., Kim, W.G., Yoon, Y., Kang, J.-W., Hong, Y.M., Kim, H.W., 2012. Removal of amoxicillin by UV and UV/H_2O_2. Sci. Total. Environ. 420, 160–167.
Karlesa, A., De Vera, G.A.D., Dodd, M.C., Park, J., Espino, M.P.B., Lee, Y., 2014. Ferrate(VI) oxidation of beta-lactam antibiotics: reaction kinetics, antibacterial activity changes, and transformation products. Environ. Sci. Technol. 48 (17), 10380–10389.
Kerkaert, B., Mestdagh, F., Cucu, T., Aedo, P.R., Ling, S.Y., De Meulenaer, B., 2011. Hypochlorous and peracetic acid induced oxidation of dairy proteins. J. Agr. Food Chem. 59 (3), 907–914.
Kitis, M., 2004. Disinfection of wastewater with peracetic acid: a review. Environ. Int. 30 (1), 47–55.
Koivunen, J., Heinonen–Tanski, H., 2005. Inactivation of enteric microorganisms with chemical disinfectants, UV irradiation and combined chemical/UV treatments. Water Res. 39, 1519–1526.
Kolpin, D.W., Furlong, E.T., Meyer, M.T., Thurman, E.M., Zaugg, S.D., Barber, L.B., Buxton, H.T., 2002. Pharmaceuticals, hormones, and other organic wastewater contaminants in US streams, 1999-2000: a national reconnaissance. Environ. Sci. Technol. 36 (6), 1202–1211.
Kummerer, K., 2001. Drugs in the environment: emission of drugs, diagnostic aids and disinfectants into wastewater by hospitals in relation to other sources - a review. Chemosphere 45 (6–7), 957–969.
Kummerer, K., 2004. Resistance in the environment. J. Antimicrob. Chemother. 54 (2), 311–320.
Liberti, L., Notarnicola, M., 1999. Advanced treatment and disinfection for municipal wastewater reuse in agriculture. Water Sci. Technol. 40 (4–5), 235–245.
Lubello, C., Caretti, C., Gori, R., 2002. Comparison between PAA/UV and H2O2/UV disinfection for wastewater reuse. Water Sci. Technol. Water Suppl. 2 (1), 205–212.
Luukkonen, T., Pehkonen, S., 2017. Peracids in water treatment: a critical review. Crit. Rev. Environ. Sci. Technol. 1, 1–39.
Monarca, S., Richardson, S.D., Feretti, D., Grottolo, M., Thruston, A.D., Zani, C., Navazio, G., Ragazzo, P., Zerbini, I., Alberti, A., 2002. Mutagenicity and disinfection by-products in surface drinking water disinfected with peracetic acid. Environ. Toxicol. Chem. 21 (2), 309–318.
Navalon, S., Alvaro, M., Garcia, H., 2008. Reaction of chlorine dioxide with emergent water pollutants: product study of the reaction of three beta-lactam antibiotics with ClO_2. Water Res. 42 (8–9), 1935–1942.
Pedersen, P.O., Brodersen, E., Cecil, D., 2013. Disinfection of tertiary wastewater effluent prior to river discharge using peracetic acid; treatment efficiency and results on by-products formed in full scale tests. Water Sci. Technol. 68 (8), 1852–1856.
Rickman, K.A., Mezyk, S.P., 2010. Kinetics and mechanisms of sulfate radical oxidation of β-lactam antibiotics in water. Chemosphere 81 (3), 359–365.
Rossi, S., Antonelli, M., Mezzanotte, V., Nurizzo, C., 2007. Peracetic acid disinfection: a feasible alternative to wastewater chlorination. Water Environ. Res. 79 (4), 341–350.
Santos, L.H., Araújo, A.N., Fachini, A., Pena, A., Delerue-Matos, C., Montenegro, M.C.B.S.M., 2010. Ecotoxicological aspects related to the presence of pharmaceuticals in the aquatic environment. J. Hazard. Mater. 175 (1), 45–95.
Sharma, V.K., Chen, L., Zboril, R., 2016. Review on high valent Fe^{VI} (ferrate): a sustainable green oxidant in organic chemistry and transformation of pharmaceuticals. ACS Sustan. Chem. Eng. 4, 18–34.
Sharma, V.K., Liu, F., Tolan, S., Sohn, M., Kim, H., Oturan, M.A., 2013. Oxidation of β-lactam antibiotics by ferrate(VI). Chem. Eng. J. 221 (1), 446–451.
Veschetti, E., Cutilli, D., Bonadonna, L., Briancesco, R., Martini, C., Cecchini, G., Anastasi, P., Ottaviani, M., 2003. Pilot-plant comparative study of peracetic acid and sodium hypochlorite wastewater disinfection. Water Res. 37, 78–94.
Yuan, Z., Ni, Y., van Heiningen, A.R.P., 1997a. Kinetics of peracetic acid decomposition. Part I: spontaneous decomposition at typical pulp bleaching conditions. Can. J. Chem. Eng. 75, 37–41.
Yuan, Z., Ni, Y., van Heiningen, A.R.P., 1997b. Kinetics of peracetic acid decomposition. Part II: pH effect and alkaline hydrolysis. Can. J. Chem. Eng. 75, 42–47.
Zhao, X., Zhang, T., Zhou, Y., Liu, D., 2007. Preparation of peracetic acid from hydrogen peroxide Part I: kinetics for peracetic acid synthesis and hydrolysis. J. Mol. Cata. 271, 246–252.
Zhou, F., Lu, C., Yao, Y., Sun, L., Gong, F., Li, D., Pei, K., Lu, W., Chen, W., 2015. Activated carbon fibers as an effective metal-free catalyst for peracetic acid activation: implications for the removal of organic pollutants. Chem. Eng. J. 281, 953–960.

Supplementary Information for

Oxidation of *β*-lactam antibiotics by peracetic acid: Reaction kinetics, product and pathway evaluation

Kejia Zhang[a,b], Xinyan Zhou[a], Penghui Du[b,c], Tuqiao Zhang[a], Meiquan Cai[b,d], Peizhe Sun[b,e], Ching-Hua Huang[b,*]

[a] *College of Civil Engineering and Architecture, Zhejiang University, Hangzhou 310058, People's Republic of China*

[b] *School of Civil and Environmental Engineering, Georgia Institute of Technology, Atlanta, Georgia 30332, United States*

[c] *Institute of Process Engineering, Chinese Academy of Sciences, Beijing 100190, People's Republic of China*

[d] *School of Environment, Tsinghua University, Beijing 100084, People's Republic of China*

[e] *School of Environmental Science and Engineering, Tianjin University, Tianjin 300072, People's Republic of China*

* Corresponding author. Tel: +1 4048947694; fax: +1 4043857087.

Email address: ching-hua.huang@ce.gatech.edu (C.-H. Huang).

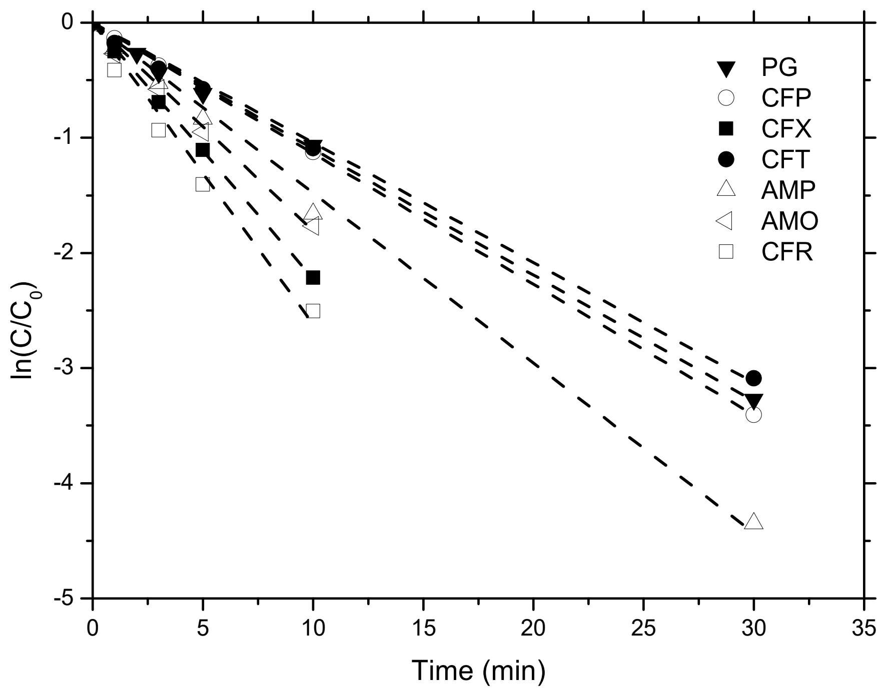

Fig. S1 - Relationships between ln([β-lactam]/[β-lactam]$_0$) and reaction time

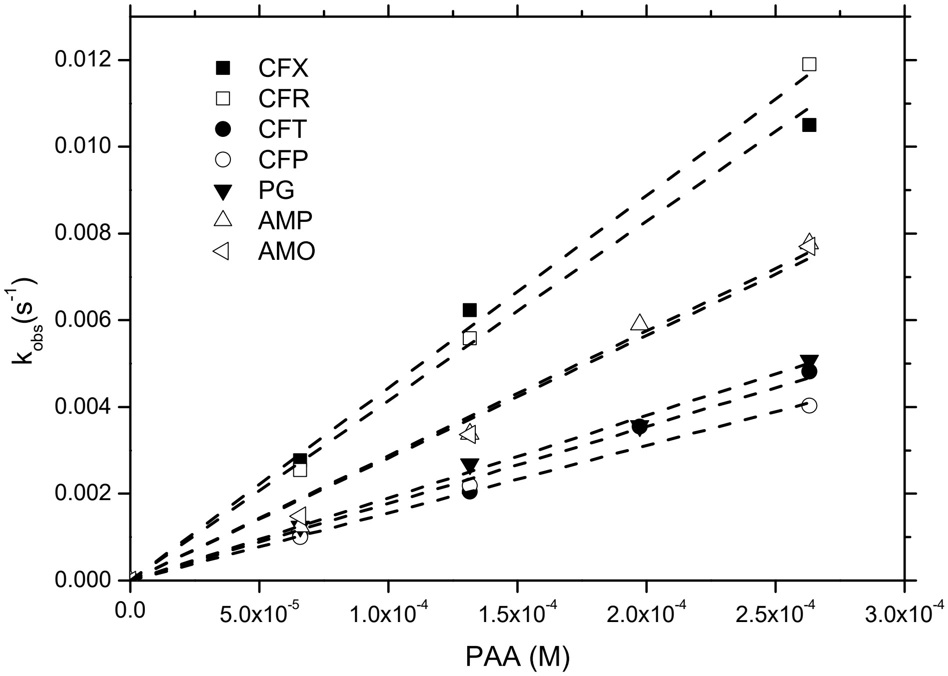

Fig. S2 - Relationships between the pseudo-first-order rate constants for degradation of β-lactams and initial PAA concentration

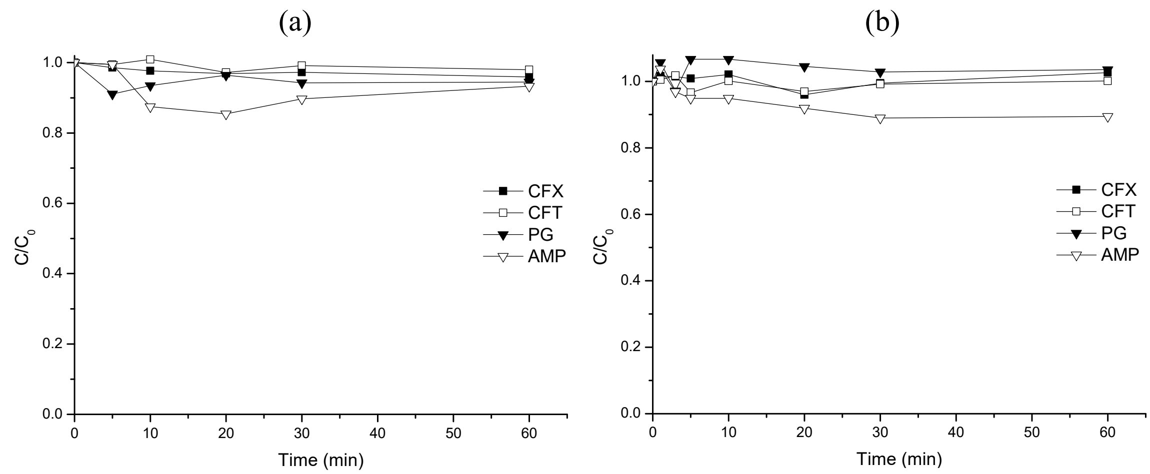

Fig. S3 - Degradation of β-lactam antibiotics by 33 μM of H_2O_2 only at pH 5 (a) and pH 7 (b). Initial β-lactam concertation was 10 μM.

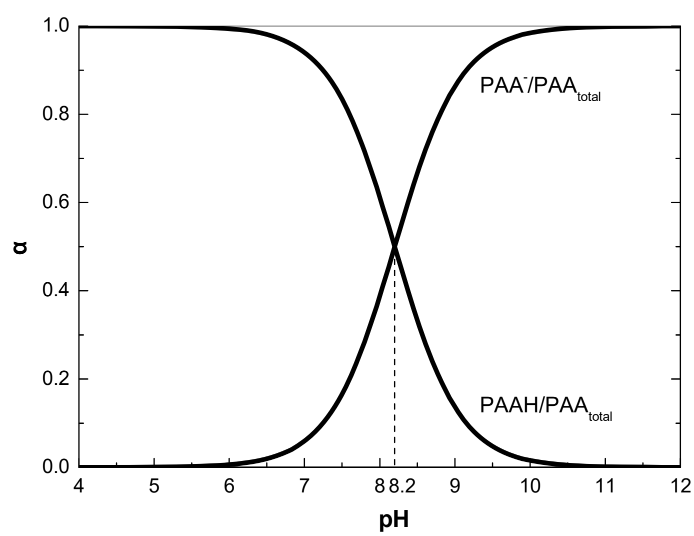

Fig. S4 - Relationships between pH, peracetic acid, and the peracetate ion ($PAA_{total} = PAA^- + PAAH$, α is the fraction of the PAA species)

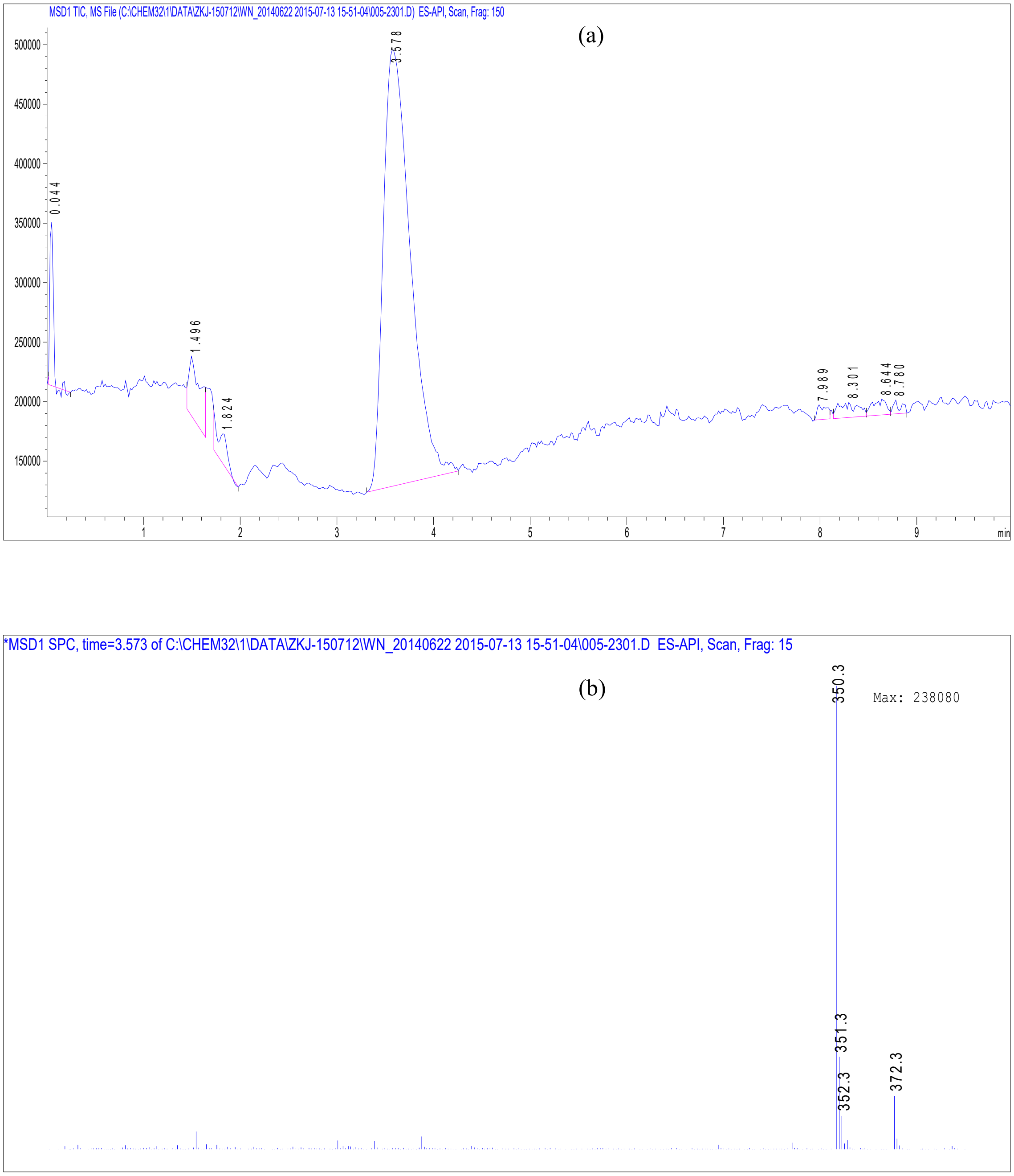

Fig. S5 – Sample analysis of reaction of AMP with PAA at the initial reaction time: (a) HPLC/MS chromatogram and (b) mass spectrum of retention time (RT) = 3.573 min.

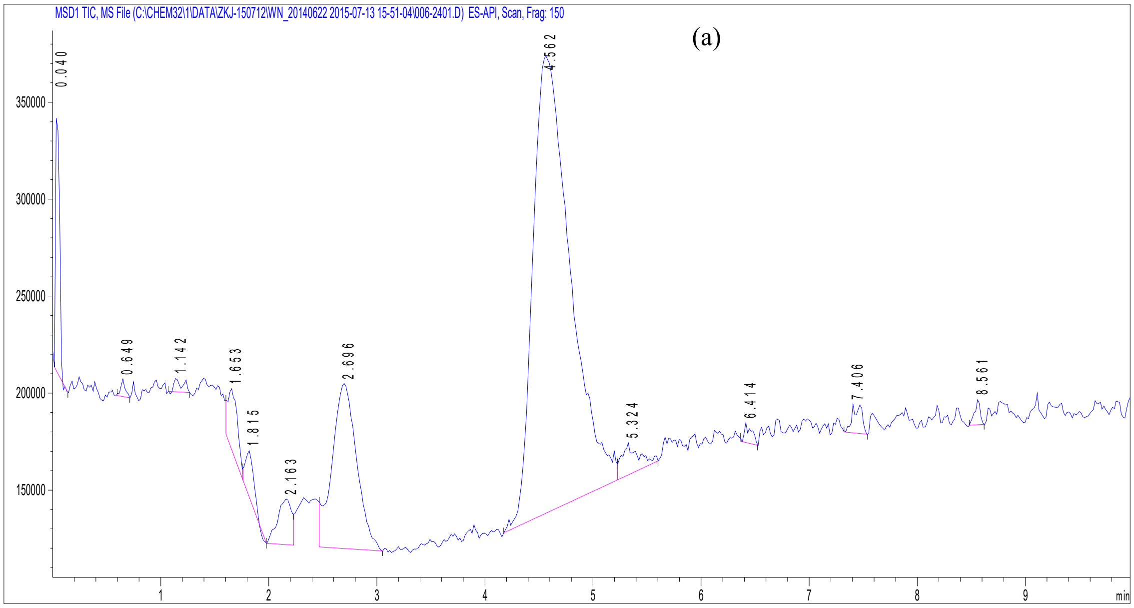

MSD1 TIC, MS File (C:\CHEM32\1\DATA\ZKJ-150712\WN_20140622 2015-07-13 15-51-04\006-2401.D) ES-API, Scan, Frag: 150
(a)
0.040
0.649
1.142
1.653
1.815
2.163
2.696
4.562
5.324
6.414
7.406
8.561
350000
300000
250000
200000
150000
1
2
3
4
5
6
7
8
9
min

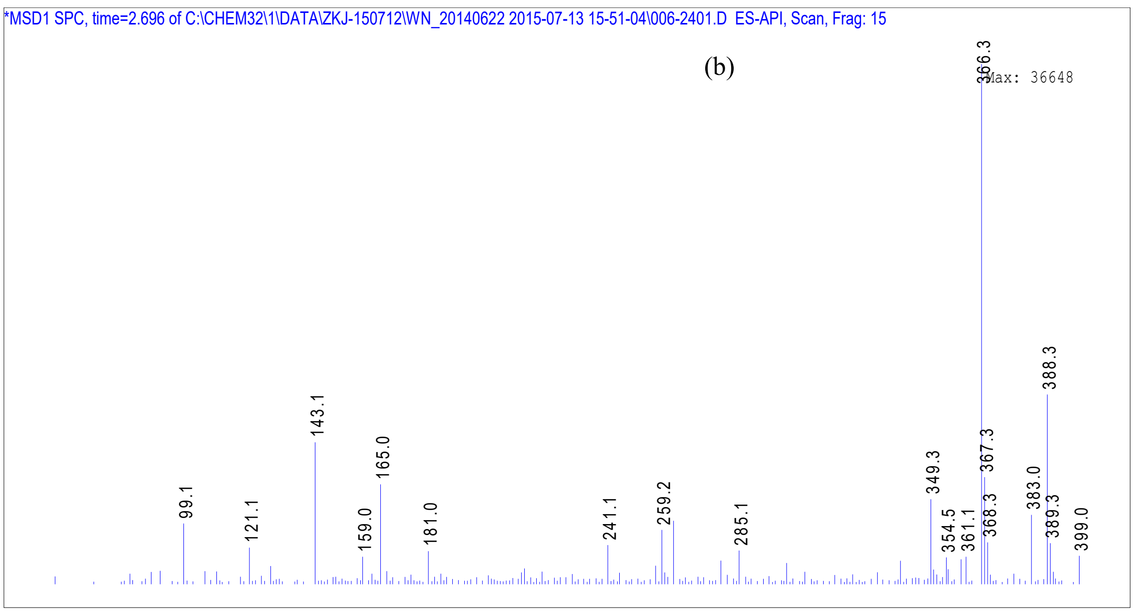

*MSD1 SPC, time=2.696 of C:\CHEM32\1\DATA\ZKJ-150712\WN_20140622 2015-07-13 15-51-04\006-2401.D ES-API, Scan, Frag: 15
(b)
366.3
Max: 36648
388.3
143.1
165.0
367.3
349.3
383.0
99.1
121.1
159.0
181.0
241.1
259.2
285.1
354.5
361.1
368.3
389.3
399.0

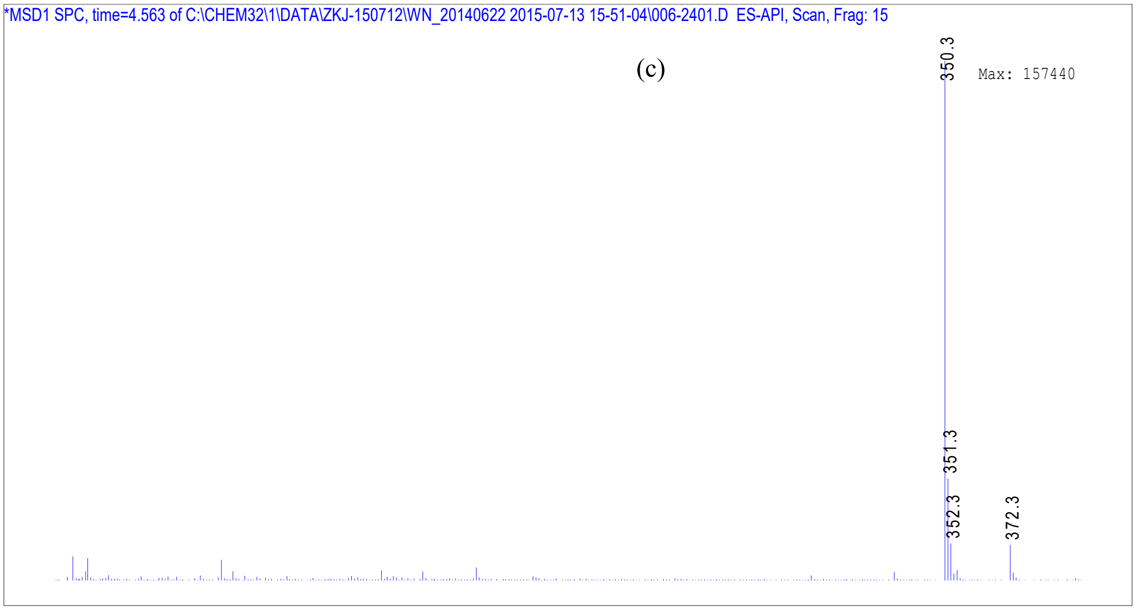

Fig. S6 – Sample analysis of reaction of AMP with PAA after 5 min: (a) HPLC/MS chromatogram, (b) mass spectrum of RT = 2.696 min, and (c) mass spectrum of RT = 4.563 min. Note: the peak at RT 4.563 min was confirmed to be AMP.

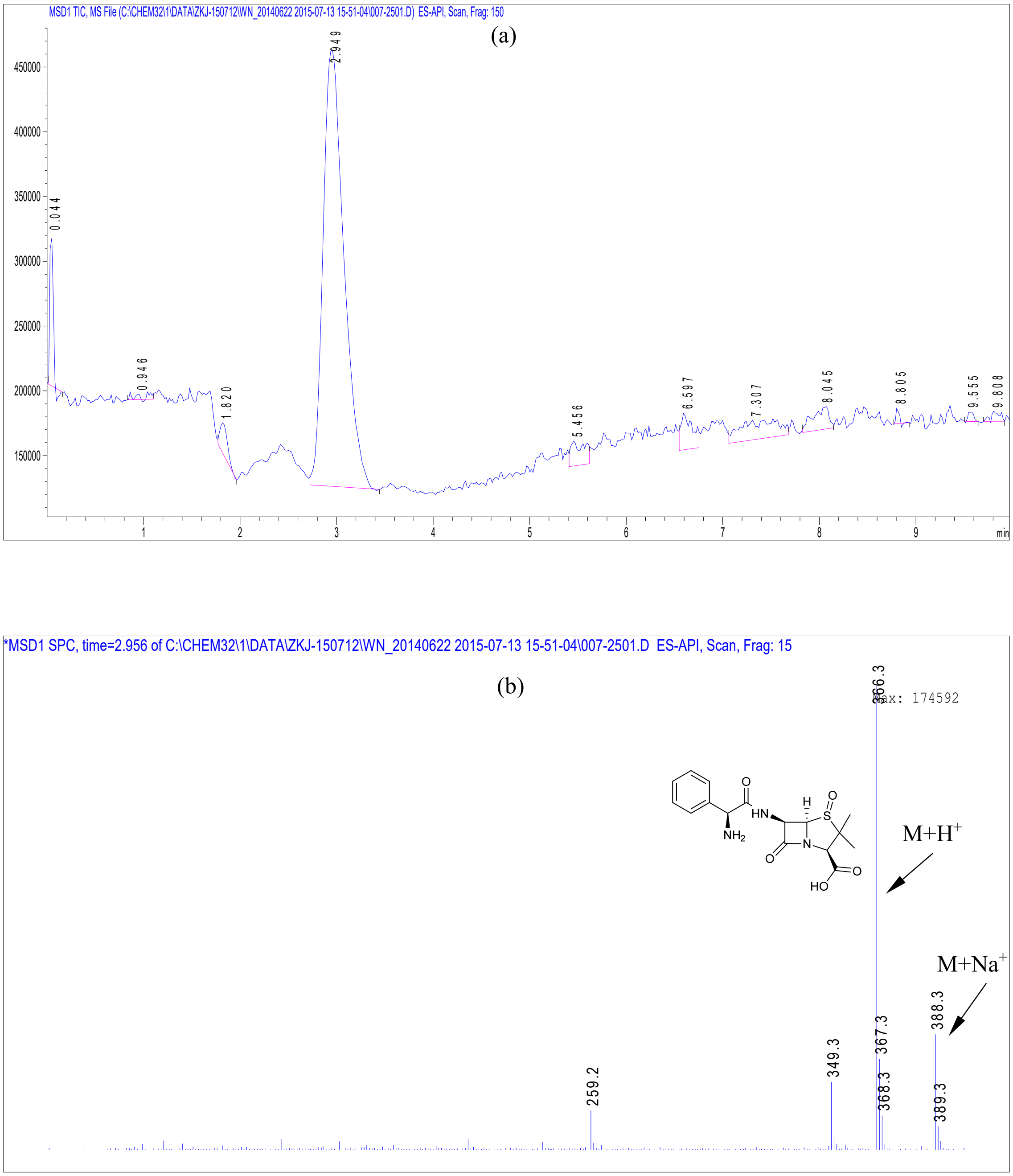

Fig. S7 - Sample analysis of reaction of AMP with PAA after 2 h: (a) HPLC/MS chromatogram, (b) mass spectrum of RT = 2.696 min.

Table S1 - Second-order rate constants of reactions of β-lactams and PAA with and without extra H_2O_2 (initial [PAA] = 131 μM, pH = 7)

Compound	k_{app} ($M^{-1}s^{-1}$) without extra H_2O_2	k_{app} ($M^{-1}s^{-1}$) with extra H_2O_2 (330 μM)	k_{app} ($M^{-1}s^{-1}$) with extra H_2O_2 (3300 μM)
Cefalexin (CFX)	42.75±1.16	44.53±1.64	44.78±1.76
Cephalothin (CFT)	15.65±0.40	18.96±0.68	20.36±0.56
Ampicillin (AMP)	25.83±0.91	33.72±0.87	N.A.
Penicillin (PG)	19.85±0.71	24.05±0.51	22.65±0.45

Table S2 - Calculated rate constants for degradation of PAA in water at 25 °C based on Yuan et al. (1997 a&b).

pH	Spontaneous Decomposition[a] k_{obs} ($M^{-1}s^{-1}$)	Hydrolysis[b] k_{obs} (s^{-1})
5	3.535×10^{-6}	2.998×10^{-9}
7	3.132×10^{-4}	2.822×10^{-7}
9	6.625×10^{-4}	4.125×10^{-6}

a: $$k_{obs} = 9.21\times10^{13}\cdot e^{-\frac{11338.71}{T}}\cdot\frac{2[\mathrm{H}^+]/K_a}{\left(1+[\mathrm{H}^+]/K_a\right)^2}$$ (Yuan et al., 1997a)

b: $$k_{obs} = \left(2.32\times10^{8}\cdot e^{-\frac{7488.68}{T}}\cdot\frac{K_a}{[\mathrm{H}^+]+K_a}+1.19\times10^{9}\cdot e^{-\frac{5903.40}{T}}\cdot\frac{[\mathrm{H}^+]}{[\mathrm{H}^+]+K_a}\right)\frac{K_w}{[\mathrm{H}^+]}$$ (Yuan et al., 1997b)

Table S3 – pKa values of β-lactams examined in this study.

Compound	M.W. (g/mol)	pK_{a1} (carboxylate group)	pK_{a2} (phenylglycine amino group)	pK_{a3} (phenol group)	Reference
Cefalexin	347.39	3.45	7.23	n/a	Est. by MarvinSketch
Cefadroxil	363.39	3.45	7.22	9.48	Est. by MarvinSketch
Cefapirin	423.47	3.54	5.0 (pyridine nitrogen)	n/a	Est. by MarvinSketch
Cephalothin	396.44	3.63	n/a	n/a	Est. by MarvinSketch
Ampicillin	349.41	2.96	9.63	n/a	Sharma et al., 2013
Amoxicillin	365.40	2.69	7.49	9.63	Sharma et al., 2013
Penicillin	334.40	2.8	n/a	n/a	Karlesa et al., 2014

n/a: not applicable

Table S4 - HOMO and LUMO energy, global nucleophilicity N index of all the seven lactams and tetracyanoethylene (TCE)

Compounds	HOMO	LUMO	N index (eV)
AMP	-0.23939	-0.02257	2.5614
AMX	-0.23078	-0.02186	2.7957
CFP	-0.24205	-0.06171	2.4890
CFR	-0.22348	-0.04776	2.9943
CFT	-0.23826	-0.05728	2.5921
CFX	-0.23271	-0.04784	2.7431
PG	-0.23915	-0.02045	2.5679
TCE	-0.33520	-0.18225	0

Table S5 - Cartesian coordinate of CFX

Center number	Atom number	Coordinates (Angstroms) X	Y	Z
1	C	-5.6483360	0.1963130	0.5834090
2	C	-4.2181650	-0.2049820	0.3264860
3	C	-3.1937830	0.6637300	0.1605330
4	C	-3.2846460	2.1593940	0.2227030
5	O	-4.3614740	2.6637440	-0.4246720
6	O	-2.4729510	2.8551400	0.7894050
7	N	-1.8699610	0.2114970	0.0436320
8	C	-1.3780230	-1.1428860	0.2701790
9	C	-0.1198720	-0.7797510	-0.5848060
10	N	1.1734600	-0.7975760	0.0351510
11	C	2.1295780	-1.7142310	-0.3487020
12	C	3.4877690	-1.5617850	0.3727400
13	N	3.3206820	-2.0734080	1.7342110
14	C	4.0536060	-0.1464140	0.2128290
15	C	4.4626080	0.2861770	-1.0581660
16	C	4.9637610	1.5715800	-1.2457700
17	C	5.0654180	2.4506350	-0.1635710
18	C	4.6652300	2.0311970	1.1032540
19	C	4.1634980	0.7394890	1.2891680
20	O	1.9063120	-2.5971350	-1.1590730
21	C	-0.7971470	0.6041620	-0.7620320
22	O	-0.5475040	1.6225030	-1.3527130
23	S	-2.5144260	-2.3874780	-0.4513210
24	C	-4.0198680	-1.7081710	0.3557250
25	H	-5.7692720	1.2617860	0.7662270
26	H	-6.2762560	-0.0689640	-0.2765120
27	H	-6.0426410	-0.3562650	1.4454170
28	H	-4.3086140	3.6280500	-0.3064230
29	H	-1.1780560	-1.3615260	1.3225750
30	H	-0.0713270	-1.3511550	-1.5160370
31	H	1.4844130	0.0362480	0.5162760
32	H	4.1441740	-2.2590860	-0.1558150
33	H	4.2108300	-2.0625540	2.2254080
34	H	2.6736710	-1.4980630	2.2667180

35	H	4.3837580	-0.3929450	-1.9039100
36	H	5.2759730	1.8895580	-2.2361730
37	H	5.4557480	3.4532570	-0.3095500
38	H	4.7447890	2.7049610	1.9514850
39	H	3.8725810	0.4165710	2.2847540
40	H	-4.0671640	-2.0593580	1.3949520
41	H	-4.8559130	-2.1852240	-0.1666660

Table S6. Cartesian coordinate of CFR

Center	Atom	Coordinates (Angstroms)		
number	number	X	Y	Z
1	C	-5.8425745	0.5967380	0.5944210
2	C	-4.4609093	0.0576090	0.3245840
3	C	-3.3557393	0.8218341	0.1622720
4	C	-3.2970463	2.3184312	0.2382200
5	O	-4.3207403	2.9333892	-0.3995780
6	O	-2.4177862	2.9248872	0.8069111
7	N	-2.0840752	0.2411400	0.0363770
8	C	-1.7280641	-1.1564741	0.2536210
9	C	-0.4392290	-0.9131821	-0.5984800
10	N	0.8442821	-1.0529041	0.0262370
11	C	1.7141971	-2.0520112	-0.3585690
12	C	3.0781112	-2.0259612	0.3677620
13	N	2.8593602	-2.5454562	1.7196821
14	C	3.7642173	-0.6626621	0.2414450
15	C	4.2368653	-0.2396370	-1.0129321
16	C	4.8477524	0.9956481	-1.1783211
17	C	5.0017704	1.8491741	-0.0771910
18	C	4.5434423	1.4458281	1.1783371
19	C	3.9316793	0.1984220	1.3282711
20	O	1.4128361	-2.9090492	-1.1715941
21	C	-0.9795491	0.5303310	-0.7704041
22	O	-0.6321750	1.5224931	-1.3562971
23	S	-2.9823252	-2.2759532	-0.4775510
24	C	-4.4137493	-1.4582481	0.3361040
25	H	-5.8553984	1.6674571	0.7856671
26	H	-6.4995025	0.4014760	-0.2625010

27	H	-6.2841575	0.0796430	1.4556271
28	H	-4.1710923	3.8865263	-0.2739810
29	H	-1.5516891	-1.4013001	1.3044201
30	H	-0.4410590	-1.4849171	-1.5307931
31	H	1.2336111	-0.2495670	0.5021200
32	H	3.6746813	-2.7687452	-0.1700860
33	H	3.7432953	-2.6059462	2.2185912
34	H	2.2510702	-1.9305641	2.2538002
35	H	4.1203223	-0.8928101	-1.8745201
36	H	5.2119484	1.3199621	-2.1472932
37	H	4.6666284	2.0987502	2.0397692
38	H	3.5990163	-0.1069470	2.3163212
39	H	-4.4988553	-1.8153581	1.3709101
40	H	-5.2922234	-1.8430251	-0.1928720
41	O	5.6113764	3.0503032	-0.2963810
42	H	5.6384924	3.5499363	0.5302420

Table S7. Cartesian coordinate of CFT

Center	Atom	Coordinates (Angstroms)		
number	number	X	Y	Z
1	C	4.2921693	-0.1105390	0.0155190
2	C	2.8354422	-0.2935530	-0.3098780
3	C	1.9295781	-0.7705401	0.5757230
4	C	2.2041172	-1.1486271	2.0052202
5	O	3.3074183	-1.9168421	2.1494372
6	O	1.5063491	-0.8041871	2.9297582
7	N	0.5727530	-0.8490791	0.2501280
8	C	-0.0790270	-0.3154140	-0.9430181
9	C	-1.2511571	-1.3220981	-0.6978231
10	N	-2.5663932	-0.8189791	-0.4540910
11	C	-3.6141623	-1.1073041	-1.2905881
12	C	-4.9911794	-0.5896010	-0.8367811
13	O	-3.4912933	-1.7644161	-2.3122022
14	C	-0.4231330	-1.7973221	0.5267050
15	O	-0.5296740	-2.6389212	1.3785161
16	S	0.9452841	-0.5907200	-2.4363032
17	C	2.4628052	0.1547950	-1.7095091

18	O	4.6214624	1.2761461	-0.2668180
19	C	5.9330935	1.5972771	-0.1266040
20	C	6.1630705	3.0586202	-0.4265090
21	O	6.7807035	0.7986221	0.2028990
22	H	4.5381403	-0.3390460	1.0501791
23	H	4.9164794	-0.7501411	-0.6194820
24	H	3.3933853	-2.0887902	3.1035592
25	H	-0.3476610	0.7402441	-0.8471311
26	H	-1.3198731	-2.0863462	-1.4768851
27	H	-2.7565822	-0.2896760	0.3865450
28	H	-5.5241714	-0.3220360	-1.7530661
29	H	-5.5182594	-1.4563181	-0.4201100
30	H	2.3857692	1.2467221	-1.7419841
31	H	3.2689753	-0.1170140	-2.3983172
32	H	5.6111364	3.6763243	0.2882710
33	H	7.2278646	3.2778763	-0.3584540
34	H	5.7917855	3.3038253	-1.4254391
35	C	-5.0091664	0.5231910	0.1699430
36	C	-5.1068314	0.4319030	1.5367311
37	S	-4.8435584	2.1965262	-0.3150740
38	C	-5.0516494	1.6959221	2.2003822
39	H	-5.2262164	-0.5152550	2.0526322
40	C	-4.9109584	2.7409072	1.3316641
41	H	-5.1196884	1.8172111	3.2751622
42	H	-4.8510284	3.7970153	1.5544931

Table S8. Cartesian coordinate of CFP

Center number	Atom number	Coordinates (Angstroms) X	Y	Z
1	C	-4.3190023	0.5997440	1.0450531
2	C	-2.9087382	0.0527050	1.0541051
3	C	-2.4152292	-0.6824781	0.0320070
4	C	-3.1737132	-1.0556271	-1.2108121
5	O	-4.4307643	-1.4767561	-0.9514321
6	O	-2.7050442	-0.9974281	-2.3229502
7	N	-1.0648911	-1.0404991	-0.0156030
8	C	-0.0028220	-0.5516220	0.8562711

9	C	0.8452971	-1.8002991	0.4450970
10	N	2.0916702	-1.6068281	-0.2314020
11	C	3.2840183	-1.9104231	0.3622510
12	C	4.5392623	-1.7139701	-0.4970050
13	S	4.5286503	-0.3653640	-1.7314271
14	O	3.3806533	-2.3528372	1.4976321
15	C	-0.3835450	-2.1953622	-0.4200140
16	O	-0.6828721	-3.1128582	-1.1360821
17	S	-0.5565730	-0.4799210	2.6022842
18	C	-2.0863222	0.4768160	2.2515312
19	O	-4.4887573	1.4221541	-0.1335380
20	C	-5.7715344	1.7503781	-0.4383860
21	C	-5.8224224	2.5830632	-1.6960791
22	O	-6.7224875	1.4134631	0.2298950
23	C	4.5390383	1.1136391	-0.7346911
24	C	4.5166023	1.1435621	0.6636531
25	C	4.5292613	2.3879472	1.2988041
26	N	4.5592493	3.5633533	0.6632161
27	C	4.5811283	3.5159093	-0.6761961
28	C	4.5728793	2.3380352	-1.4171621
29	H	-5.0702204	-0.1917720	1.0362481
30	H	-4.4938463	1.2191441	1.9303481
31	H	-4.8332254	-1.6774411	-1.8136691
32	H	0.4047190	0.4121580	0.5388790
33	H	1.0088011	-2.4895422	1.2772771
34	H	2.1036052	-1.2049691	-1.1603771
35	H	5.3911284	-1.6188771	0.1778500
36	H	4.6931904	-2.6195522	-1.0937351
37	H	-1.8459611	1.5453461	2.1724222
38	H	-2.6906562	0.3643070	3.1586132
39	H	-5.3205174	2.0629122	-2.5166292
40	H	-6.8613585	2.7832752	-1.9551152
41	H	-5.2924604	3.5270823	-1.5375971
42	H	4.4857183	0.2433290	1.2656921
43	H	4.5119993	2.4294082	2.3864052
44	H	4.6076034	4.4746943	-1.1906121
45	H	4.5952823	2.3748632	-2.5019532

Table S9. Cartesian coordinate of PG

Center number	Atom number	Coordinates (Angstroms) X	Y	Z
1	C	2.9040572	0.4543580	0.5003410
2	C	3.3723433	1.9041321	0.4265920
3	O	2.4318842	2.7598742	-0.0167560
4	O	4.4985873	2.2440242	0.7190071
5	N	1.4643941	0.2634300	0.4518860
6	C	0.9183441	-0.7160511	-0.4995690
7	C	-0.1019400	-1.1646411	0.6018630
8	N	-1.5021631	-0.9577831	0.3950630
9	C	-2.3807402	-2.0105212	0.3332600
10	C	-3.8703883	-1.6479461	0.2156480
11	C	-4.2165683	-0.2126630	-0.1089680
12	C	-4.3757043	0.7378211	0.9108951
13	C	-4.6733194	2.0679942	0.6095340
14	C	-4.8194874	2.4686812	-0.7191421
15	C	-4.6656984	1.5324071	-1.7435311
16	C	-4.3648383	0.2048370	-1.4398041
17	O	-2.0199782	-3.1762972	0.3937410
18	C	0.6586521	-0.1626160	1.5118321
19	O	0.6535811	0.1399290	2.6779502
20	S	2.3292272	-1.8300571	-0.8781801
21	C	3.5322243	-0.4051890	-0.6690151
22	C	4.9060064	-0.9495841	-0.2662580
23	C	3.6285053	0.3857930	-1.9854052
24	H	3.2791412	0.0777920	1.4584981
25	H	2.8525272	3.6372613	-0.0254720
26	H	0.4808980	-0.2845910	-1.4031251
27	H	0.0452150	-2.2020572	0.9110061
28	H	-1.8700521	-0.0172970	0.3596780
29	H	-4.3197253	-1.9450271	1.1705021
30	H	-4.2730713	0.4305400	1.9488211
31	H	-4.7970704	2.7877762	1.4132801
32	H	-5.0558604	3.5019633	-0.9548721
33	H	-4.7831444	1.8350871	-2.7800052
34	H	-4.2489533	-0.5201300	-2.2415872

35	H	5.5787234	-0.1137600	-0.0515420
36	H	4.8382544	-1.5795141	0.6247120
37	H	5.3407544	-1.5415581	-1.0769071
38	H	4.3648543	1.1918961	-1.8941381
39	H	3.9510243	-0.2765580	-2.7917342
40	H	2.6703152	0.8288791	-2.2705312
41	H	-4.2783713	-2.3304362	-0.5355300

Table S10. Cartesian coordinate of AMP

Center number	Atom number	Coordinates (Angstroms) X	Y	Z
1	C	3.1882382	0.2447540	0.5212210
2	C	3.7725853	1.6410271	0.7101011
3	O	2.8671922	2.6312682	0.5985990
4	O	4.9508134	1.8346021	0.9189291
5	N	1.7394021	0.1610640	0.6017190
6	C	1.0195201	-0.5474200	-0.4676390
7	C	0.0713770	-1.1552281	0.6220560
8	N	-1.3133721	-0.7898611	0.6320700
9	C	-2.3077612	-1.6925761	0.3568280
10	C	-3.7605473	-1.1797741	0.5589360
11	N	-4.7510984	-2.1100402	0.0221670
12	C	-3.9766693	0.2286610	0.0302350
13	C	-4.4831863	1.2357081	0.8595941
14	C	-4.7035384	2.5234392	0.3664850
15	C	-4.4219723	2.8192642	-0.9670051
16	C	-3.9157963	1.8225581	-1.8048541
17	C	-3.6920123	0.5393400	-1.3086631
18	O	-2.0768662	-2.8536142	0.0466570
19	C	1.0113761	-0.4412050	1.6315341
20	O	1.1527101	-0.4140990	2.8273662
21	S	2.2840302	-1.6424761	-1.2271391
22	C	3.6148043	-0.3661350	-0.8724421
23	C	4.9763984	-1.0595351	-0.7714861
24	C	3.6240273	0.6896381	-1.9912051
25	H	3.6231713	-0.3626670	1.3227831
26	H	3.3599853	3.4597713	0.7313921

27	H	0.5384110	0.0995580	-1.2051201
28	H	0.1393410	-2.2434822	0.6794471
29	H	-1.5728791	0.1650480	0.8367441
30	H	-3.8886343	-1.1505331	1.6513641
31	H	-4.8137074	-1.9813121	-0.9858891
32	H	-4.3823513	-3.0524192	0.1514850
33	H	-4.7164704	1.0061001	1.8958181
34	H	-5.0990854	3.2918623	1.0240811
35	H	-4.5943313	3.8196953	-1.3525261
36	H	-3.6918433	2.0461842	-2.8438312
37	H	-3.2878023	-0.2275530	-1.9656772
38	H	5.7338074	-0.3299000	-0.4697010
39	H	4.9578844	-1.8663561	-0.0339320
40	H	5.2690404	-1.4799031	-1.7380051
41	H	4.4230203	1.4199461	-1.8217751
42	H	3.8060333	0.2070250	-2.9539362
43	H	2.6755412	1.2300571	-2.0547732

Table S11. Cartesian coordinate of AMX

Center number	Atom number	Coordinates (Angstroms) X	Y	Z
1	C	3.3863203	0.3012910	0.5337870
2	C	3.8529643	1.7049361	0.9061961
3	O	2.8644992	2.6187292	0.9370821
4	O	5.0145344	1.9707241	1.1285301
5	N	1.9538701	0.0762590	0.6305600
6	C	1.2622221	-0.5334640	-0.5148780
7	C	0.4055320	-1.3722851	0.4942010
8	N	-1.0047981	-1.1418241	0.5806780
9	C	-1.9230411	-2.0907022	0.2107800
10	C	-3.4082463	-1.7418781	0.5035410
11	N	-4.3277603	-2.6883472	-0.1254310
12	C	-3.7656813	-0.3058280	0.1629550
13	C	-4.3886233	0.5248900	1.0993101
14	C	-4.7490674	1.8341231	0.7794891
15	C	-4.4923743	2.3336812	-0.5004430
16	C	-3.8699633	1.5168961	-1.4529091

17	C	-3.5134683	0.2161680	-1.1170761
18	O	-1.5984411	-3.1774232	-0.2491840
19	C	1.3120831	-0.7266851	1.5776491
20	O	1.4878831	-0.8547641	2.7623642
21	S	2.5901322	-1.3920891	-1.4508051
22	C	3.8193983	-0.0679460	-0.9414641
23	C	5.2371064	-0.6465380	-0.9649541
24	C	3.7069833	1.1321881	-1.8974041
25	H	3.8989563	-0.3689490	1.2326721
26	H	3.2878073	3.4620603	1.1747391
27	H	0.7042081	0.1665430	-1.1414701
28	H	0.5708670	-2.4469942	0.3941310
29	H	-1.3439781	-0.2470930	0.9053861
30	H	-3.5036853	-1.8600921	1.5936041
31	H	-4.4389283	-2.4366702	-1.1058111
32	H	-3.8688853	-3.5995973	-0.1306890
33	H	-4.6050504	0.1428560	2.0932132
34	H	-5.2330464	2.4630692	1.5235051
35	H	-3.6744233	1.9188791	-2.4413042
36	H	-3.0247252	-0.4045240	-1.8645911
37	H	5.9388545	0.0967220	-0.5746090
38	H	5.3094504	-1.5483671	-0.3510930
39	H	5.5355544	-0.8983481	-1.9867602
40	H	4.4463243	1.8980981	-1.6383781
41	H	3.9012703	0.8082471	-2.9221952
42	H	2.7149302	1.5908661	-1.8665891
43	O	-4.8171324	3.6034493	-0.8800821
44	H	-5.2504134	4.0552953	-0.1438950

Table S12. Cartesian coordinate of CFXN model compound

Center number	Atom number	Coordinates (Angstroms) X	Y	Z
1	C	-5.1068360	0.3684570	1.3364470
2	C	-3.7522370	-0.1135660	0.8831890
3	C	-2.9049440	0.5973460	0.1030530
4	C	-3.1440850	1.9796240	-0.4279210
5	O	-4.3982380	2.1673020	-0.9024230

6	O	-2.3000400	2.8463520	-0.4401380
7	N	-1.6115490	0.1308360	-0.1784230
8	C	-0.9335930	-1.0042160	0.4358700
9	C	0.0280680	-1.0407360	-0.7975670
10	N	1.4262440	-0.8157710	-0.5994270
11	C	2.3610560	-1.7648910	-0.9308030
12	C	3.8335340	-1.3448950	-0.7893050
13	C	4.1258330	-0.0845250	-0.0071680
14	C	4.1518820	1.1672520	-0.6405580
15	C	4.3940180	2.3332100	0.0882480
16	C	4.6186770	2.2647340	1.4636510
17	C	4.5989760	1.0247990	2.1055220
18	C	4.3522230	-0.1378580	1.3759860
19	O	2.0588620	-2.8749890	-1.3418950
20	C	-0.8219230	0.1440570	-1.3338350
21	O	-0.8468270	0.8157100	-2.3315200
22	S	-2.0706070	-2.4309780	0.6231810
23	C	-3.3895830	-1.4660680	1.4654770
24	H	-5.2926870	1.4128850	1.0960030
25	H	-5.8983960	-0.2289450	0.8667780
26	H	-5.2088680	0.2327370	2.4204790
27	H	-4.4260470	3.0909710	-1.2069370
28	H	-0.4598340	-0.7602870	1.3909840
29	H	-0.0866340	-1.9472090	-1.3977340
30	H	1.7464060	0.0944310	-0.2984580
31	H	4.2133730	-1.2581590	-1.8142070
32	H	3.9874740	1.2273920	-1.7137010
33	H	4.4119140	3.2923990	-0.4205810
34	H	4.8110600	3.1703520	2.0310090
35	H	4.7780200	0.9624780	3.1750020
36	H	4.3398800	-1.1003320	1.8813700
37	H	-3.1347020	-1.3483620	2.5269930
38	H	-4.2724050	-2.1135560	1.4332090
39	H	4.3418400	-2.2079550	-0.3500450

Table S13. Cartesian coordinate of PAA

Center number	Atom number	Coordinates (Angstroms) X	Y	Z
1	C	0.5405790	1.3739490	0.0116960
2	H	0.0317600	1.7454410	-0.8817170
3	H	1.5641780	1.7449190	0.0443090
4	H	-0.0247240	1.7346370	0.8742870
5	C	0.5954880	-0.1291980	0.0028830
6	O	1.5869320	-0.8122970	0.0102170
7	O	-0.6002450	-0.8162340	-0.0269600
8	O	-1.7430720	0.0923460	-0.0641810
9	H	-2.3365360	-0.4040260	0.5230270

References

MarvinSketch, version 15.4.27.0, by ChemAxon Ltd. 2015. http://www.chemaxon.com.

Karlesa, A., De Vera, G.A.D., Dodd, M.C., Park, J., Espino, M.P.B., Lee, Y., 2014. Ferrate(VI) oxidation of beta-lactam antibiotics: Reaction kinetics, antibacterial activity changes, and transformation products. Environ. Sci. Technol. 48(17), 10380-10389.

Sharma, V.K., Liu, F., Tolan, S., Sohn, M., Kim, H., Oturan, M.A., 2013. Oxidation of β-lactam antibiotics by ferrate(VI). Chem. Eng. J. 221(1), 446-451.

Yuan, Z., Ni, Y., van Heiningen, A.R.P., 1997a. Kinetics of peracetic acid decomposition. Part I: Spontaneous decomposition at typical pulp bleaching conditions. Can. J. Chem. Eng. 75, 37-41.

Yuan, Z., Ni, Y., van Heiningen, A.R.P., 1997b. Kinetics of peracetic acid decomposition. Part II: pH effect and alkaline hydrolysis. Can. J. Chem. Eng. 75, 42-47.